Published online: April 12, 2019

Article

SOURCE DATA | TRANSPARENT PROCESS

THE EMBO JOURNAL

Regulation of death receptor signaling by the autophagy protein TP53INP2

Saška Ivanova[1,2,3,*], Mira Polajnar[4,5,6], Alvaro Jesus Narbona-Perez[1], Maria Isabel Hernandez-Alvarez[1,3,7], Petra Frager[1], Konstantin Slobodnyuk[1], Natalia Plana[1], Angel R Nebreda[1,8], Manuel Palacin[1,2,9], Roger R Gomis[1,8,10,11], Christian Behrends[4,6] & Antonio Zorzano[1,2,3,**]

Abstract

TP53INP2 positively regulates autophagy by binding to Atg8 proteins. Here, we uncover a novel role of TP53INP2 in death-receptor signaling. TP53INP2 sensitizes cells to apoptosis induced by death receptor ligands. In keeping with this, TP53INP2 deficiency in cultured cells or mouse livers protects against death receptor-induced apoptosis. TP53INP2 binds caspase-8 and the ubiquitin ligase TRAF6, thereby promoting the ubiquitination and activation of caspase-8 by TRAF6. We have defined a TRAF6-interacting motif (TIM) and a ubiquitin-interacting motif in TP53INP2, enabling it to function as a scaffold bridging already ubiquitinated caspase-8 to TRAF6 for further polyubiquitination of caspase-8. Mutations of key TIM residues in TP53INP2 abrogate its interaction with TRAF6 and caspase-8, and subsequently reduce levels of death receptor-induced apoptosis. A screen of cancer cell lines showed that those with higher protein levels of TP53INP2 are more prone to TRAIL-induced apoptosis, making TP53INP2 a potential predictive marker of cancer cell responsiveness to TRAIL treatment. These findings uncover a novel mechanism for the regulation of caspase-8 ubiquitination and reveal TP53INP2 as an important regulator of the death receptor pathway.

Keywords apoptosis; death receptor signaling; TP53INP2; TRAF6 ubiquitination

Subject Categories Cancer; Autophagy & Cell Death

DOI 10.15252/embj.201899300 | Received 22 February 2018 | Revised 15 February 2019 | Accepted 12 March 2019

The EMBO Journal (2019) e99300

Introduction

Apoptosis is a process of programmed cell death that is crucial for the homeostasis of an organism, and its deregulation occurs in several pathologies (Jacobson *et al*, 1999; Vaux & Korsmeyer, 1999). Apoptosis can be triggered through either an intrinsic or extrinsic pathway (Ferri & Kroemer, 2001; Fulda & Debatin, 2006). In the former, cellular damage is sensed by various Bcl-2 pro-apoptotic homologues and leads to Bax/Bak oligomerization in the outer mitochondrial membrane, release of cytochrome c, and apoptosome formation, where caspase-9 is activated (Zou *et al*, 1999). Activated caspase-9 cleaves caspases-3, -6, and -7, which execute apoptosis (Zou *et al*, 1999). In the extrinsic pathway, death ligands (FasL, TRAIL/Apo2L and TNFα) bind to their cognitive receptors and induce their trimerization, thereby allowing subsequent binding of the adaptor protein FADD and caspase-8 to the DISC complex (death-inducing signaling complex; Medema *et al*, 1997). Caspase-8 was thought to be activated through the so-called proximity-induced model, i.e., dimerization of pro-caspase-8 molecules in the DISC complex. However, this model has recently been challenged by the DED chain assembly model, which proposes that a FADD molecule interacts with several caspase-8 molecules (Dickens *et al*, 2012; Schleich *et al*, 2012). Activated caspase-8 directly cleaves executioner caspases (i.e., caspase-3) in type I cells (e.g., thymocytes), while in type II cells (e.g., hepatocytes) it cleaves the Bcl-2 homology domain 3 (BH3) protein Bid, producing tBid, which amplifies the signal through mitochondria (Li *et al*, 1998; Luo *et al*, 1998). Recently, several studies have added additional layers of complexity to caspase-8 activation, revealing that ubiquitination plays a key role in this process. For example, the E3 ubiquitin ligase cullin-3

1 Institute for Research in Biomedicine (IRB Barcelona), Barcelona Institute of Science and Technology (BIST), Barcelona, Spain
2 CIBER de Diabetes y Enfermedades Metabólicas Asociadas, Barcelona, Spain
3 Departament de Bioquimica i Biomedicina Molecular, Facultat de Biologia, Universitat de Barcelona, Barcelona, Spain
4 Institute of Biochemistry II, Goethe University School of Medicine, Frankfurt am Main, Germany
5 German Cancer Consortium (DKTK) and German Cancer Research Center (DKFZ), Heidelberg, Germany
6 Munich Cluster for System Neurology, Medical Faculty, Ludwig-Maximilians-University München, Munich, Germany
7 Hospital Universitari de Tarragona Joan XXIII, Institut Investigació Sanitaria Pere Virgili (IISPV), Universitat Rovira i Virgili, Tarragona, Spain
8 ICREA, Insitució Catalana de Recerca i Estudis Avançats, Barcelona, Spain
9 CIBER de Enfermedades Raras, Barcelona, Spain
10 CIBERONC, Barcelona, Spain
11 Departament de Medicina, Facultat de Medicina, Universitat de Barcelona, Barcelona, Spain
*Corresponding author. Tel: +34934034701; E-mail: saska.ivanova@irbbarcelona.org
**Corresponding author. Tel: +34934037197; E-mail: antonio.zorzano@irbbarcelona.org

ubiquitinates caspase-8 at its C-terminus in the DISC complex and ubiquitinated caspase-8 is aggregated by p62 for its full activation (Jin *et al*, 2009). In contrast, TRAF2 adds K48-ubiquitin chains to the large catalytic domain of caspase-8 and marks it for degradation (Gonzalvez *et al*, 2012), while HECTD3 ubiquitination of the Lys residue between the DED and the large domain of caspase-8 increases the threshold for death receptor-induced apoptosis (Li *et al*, 2013).

One of the hallmarks of cancer cells is their capacity to evade apoptosis. Most chemotherapies in clinical practice aim to induce cell death in tumors, thus shrinking the tumors to a size that can be removed by surgery, or to kill any remaining and/or circulating tumor cells. Chemotherapy has several disadvantages. In addition to not being effective in all or even in the majority of patients, it causes side effects. This observation points to the need for personalized medicine, i.e., the selection of patients that will respond and benefit from a given chemotherapy. The initial optimism caused by the discovery of TRAIL, for example, which selectively kills cancer cells, plummeted after several unsuccessful clinical trials. Thus, better antagonists and molecular markers to identify patients who would respond to TRAIL are needed (de Miguel *et al*, 2016; von Karstedt *et al*, 2017). This need is further emphasized by the observation that tumors not undergoing apoptosis upon TRAIL administration can diverge the signaling to cytokine production, thus favoring tumor growth (Hartwig *et al*, 2017; Henry & Martin, 2017).

The complexity of the cross-talk between autophagy and apoptosis has been widely studied, not only with the purpose of understanding the underlying mechanisms, but also of modulating both pathways in tumors. Several autophagic proteins have a dual role in both processes (Yousefi *et al*, 2006; Cho *et al*, 2009; Giansanti *et al*, 2011). The inhibition of autophagy causes the accumulation of autophagosomal membranes, which serve as platforms for intracellular DISC formation (Laussmann *et al*, 2011; Pan *et al*, 2011; Young *et al*, 2012; Huang *et al*, 2013). Canonical and intracellular DISC formation occurs independently and requires distinct membranes (Jiang *et al*, 2011; Laussmann *et al*, 2011; Pan *et al*, 2011; Young *et al*, 2012; Deegan *et al*, 2014). Thus, pro-caspase-8 binds to intracellular DISC on the phagophore through ATG12-ATG5-FADD on the outer membrane or through LC3-p62 on the inner membrane of the accumulating autophagosomes (Bell *et al*, 2008; Jiang *et al*, 2011; Laussmann *et al*, 2011; Pan *et al*, 2011; Young *et al*, 2012; Huang *et al*, 2013; Deegan *et al*, 2014; Tang *et al*, 2017). The LC3-p62 axis most probably recruits ubiquitinated caspase-8 in a similar way as the autophagic cargo is recruited to autophagosomes (Pankiv *et al*, 2007; Huang *et al*, 2013).

In proliferating cells, TP53INP2 is a nuclear protein that interacts with nuclear hormone receptors (Baumgartner *et al*, 2007; Francis *et al*, 2010), shuttles from the nucleus to the cytosol (Mauvezin *et al*, 2010, 2012), and stimulates protein synthesis by promoting ribosomal biogenesis in the nucleolus (Xu *et al*, 2016). However, upon nutrient depletion, TP53INP2 interacts with a nuclear and deacetylated pool of LC3 and shuttles it rapidly to the cytosol to initiate autophagy (Huang *et al*, 2015). TP53INP2 is a positive regulator of autophagy, and it interacts directly with the LIR sequence of all Atg8 family members (Nowak *et al*, 2009; Mauvezin *et al*, 2010; Sancho *et al*, 2012). We recently showed that TP53INP2 is also an ubiquitin-binding protein, with a preference for mono- and K63-linked ubiquitin chains (Sala *et al*, 2014).

Here, we identified an unexpected role of TP53INP2 in death receptor signaling. We show that TP53INP2 sensitizes various cancer cell lines to death receptor-induced apoptosis. We observed that TP53INP2 increases the activation of caspase-8 by upregulating its K63-ubiquitination levels in a TRAF6-dependent manner. Furthermore, we demonstrate that TP53INP2 acts as a scaffold for caspase-8 polyubiquitination by TRAF6. In addition, we show that cancer cell lines with high protein levels of TP53INP2 respond better to TRAIL-induced apoptosis than those with no or low amounts of TP53INP2. This observation indicates that TP53INP2 might be a potential biomarker for personalized TRAIL treatment in cancers where caspase-8 protease activity is intact. Altogether, our findings demonstrate that TP53INP2 acts as a switch at the level of caspase-8 activation, favoring death receptor-mediated apoptosis.

Results

TP53INP2 regulates death receptor-induced apoptosis

Several autophagic proteins participate in the cross-talk between autophagy and apoptosis (Yousefi *et al*, 2006; Cho *et al*, 2009; Laussmann *et al*, 2011; Huang *et al*, 2013; Strappazzon *et al*, 2016). In this regard, we examined the role of TP53INP2 in apoptosis. We overexpressed TP53INP2 in HeLa cells, which express undetectable levels of this protein, and we induced cell death by various agents. Surprisingly, TP53INP2 increased the sensitivity of cells to death induced by ligands of death receptors more efficiently than to other inducers (Fig 1A and Appendix Fig S1A). This observation prompted us to explore the role of TP53INP2 in death receptor-induced cell death. Using inhibitors of apoptosis (zVAD) and necrosis (necrostatin-1/Nec-1), annexin V staining [flow cytometry measurement of phosphatidylserine exposure (PS)] and DEVDase activity (indicative of caspase activity), we confirmed that TP53INP2 sensitizes cells to death receptor-induced apoptosis and not necroptosis (Fig 1B and C, and Appendix Fig S1B). Furthermore, the activation of caspase-8 and caspase-3, and detection of the caspase-generated 85 kDa fragment of PARP-1 were higher in cells expressing TP53INP2 and treated with a range of concentrations of FasL and TRAIL (Fig 1D and E). TNFα induces apoptosis by activation of the death receptor pathway by a process that is stimulated to cycloheximide (Kreuz *et al*, 2001), and TNFα-induced apoptosis was further augmented by TP53INP2 overexpression in HeLa cells (Appendix Fig S1C and D). Similar results were obtained in MDA231 and MCF7 cells treated with FasL (Appendix Fig S1E and F). LC3-II protein levels were increased in TP53INP2-overexpressing cells as previously described (Fig 1D and E; Sala *et al*, 2014). Moreover, time-course experiments showed that FasL-induced apoptosis in TP53INP2-expressing cells occurs faster than in control cells. In the former, apoptosis started around 4 h post-induction (Fig 1F). At this time point, caspase-3 cleavage was detected and the levels of TP53INP2 were the highest (Fig 1F), thereby supporting the notion that TP53INP2 accumulates in the first 4 h of FasL treatment and that TP53INP2 contributes to faster activation of apoptosis triggered by death receptors. Similar results were obtained by time-course experiment with TRAIL (Fig 1G). Since TP53INP2 is cleaved during apoptosis and we detected a cleavage product of approximately 26 kDa (Fig 1D–G), we explored whether the sensitization of

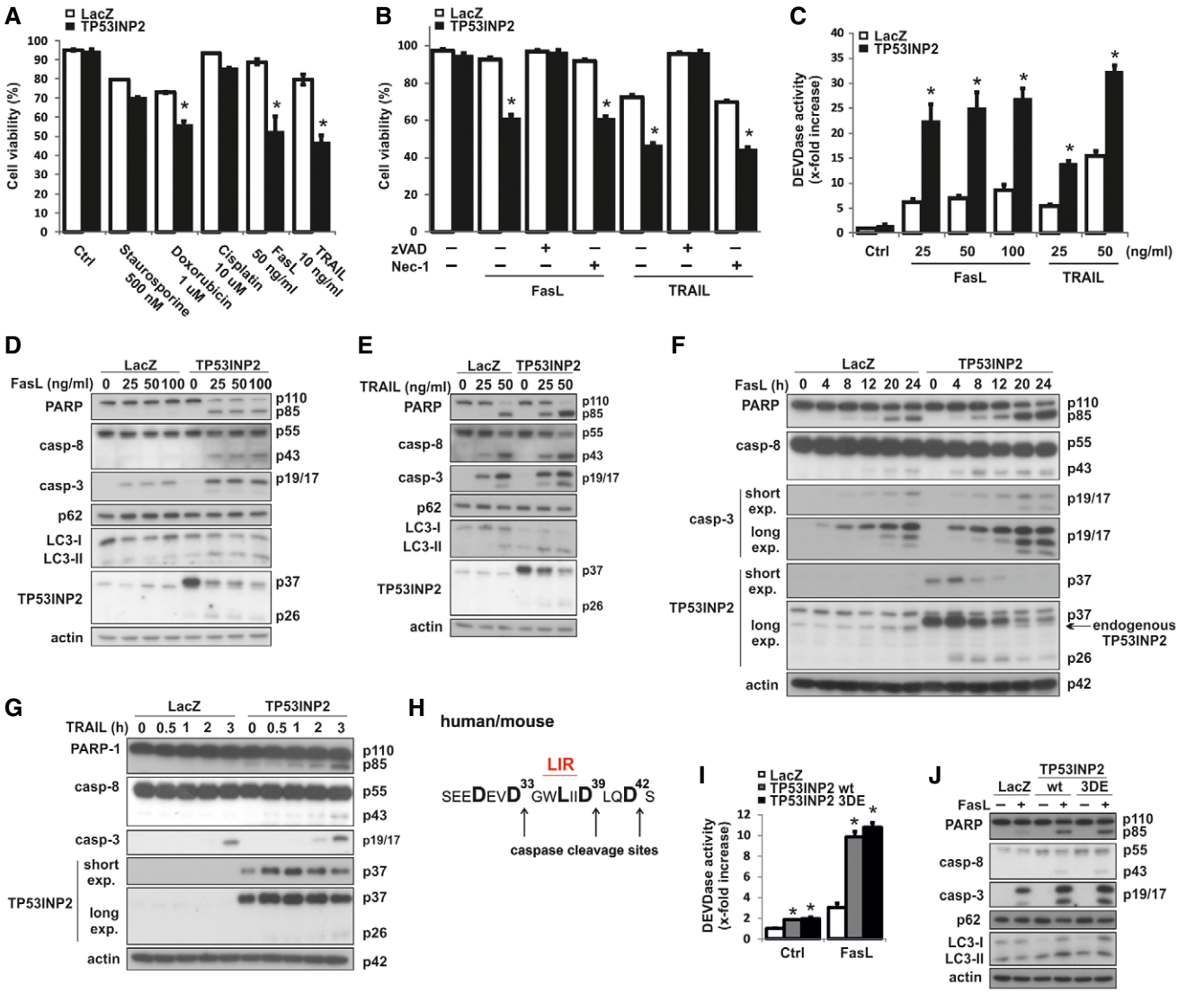

Figure 1. TP53INP2 sensitizes cells to death receptor-induced apoptosis.

A HeLa cells were treated with the indicated inducers of apoptosis for 24 h, and cell viability was assessed by annexin V and PI staining.

B The percentage of viable cells 24 h after FasL (50 ng/ml) and TRAIL (10 ng/ml) treatment in the absence or presence of z-VAD-fmk (20 μM) or Nec-1 (30 μM).

C Quantification of DEVDase activity in HeLa cells after 16 h of FasL or 4 h of TRAIL treatment.

D, E HeLa cells were infected with adenovirus for LacZ or TP53INP2 and treated with different concentrations of FasL for 16 h (D) or TRAIL for 4 h (E). Cell lysates were then subjected to Western blot analysis for various apoptotic and autophagic markers.

F Time-dependent cleavage of PARP-1, caspase-8, caspase-3, and TP53INP2 during FasL-induced apoptosis (50 ng/ml) in HeLa cells expressing LacZ or TP53INP2.

G Time-dependent cleavage of PARP-1, caspase-8, caspase-3, and TP53INP2 during TRAIL-induced apoptosis (50 ng/ml) in HeLa cells expressing LacZ or TP53INP2.

H Schematic presentation of caspase cleavage sites in human and mouse TP53INP2. LIR; LC3 interacting region.

I DEVDase activity quantification in lysates of HeLa cells expressing LacZ, wt TP53INP2 or TP53INP2 3DE mutant in control or FasL-treated cells (50 ng/ml; 16 h).

J HeLa cells were transduced with adenovirus for LacZ, wt TP53INP2 or 3DE mutant, and cell lysates were subjected to Western blot analysis with indicated antibodies.

Data information: Data are given as mean ± SEM and were analyzed by two-way Student's *t*-test; n = three independent experiments, $^*P < 0.05$.
Source data are available online for this figure.

TP53INP2 to death receptor-induced apoptosis involves its cleavage by caspases. To test this, we first mutated aspartate residues at potential caspase cleavage sites (Fig 1H) to glutamate in order to produce a caspase-noncleavable mutant form (TP53INP2 3DE). Indeed, recombinant caspase-3 cleaved the wild-type TP53INP2 but not the 3DE mutant (Appendix Fig S1G); however, the 3DE mutant did not abolish the sensitization effect of TP53INP2 to FasL-induced apoptosis (Fig 1I and J). This observation indicates that the mechanism involved does not require the cleavage of TP53INP2 by caspases.

In contrast, HeLa cells depleted of TP53INP2 by CRISPR technology were less sensitive to treatment with FasL or TRAIL

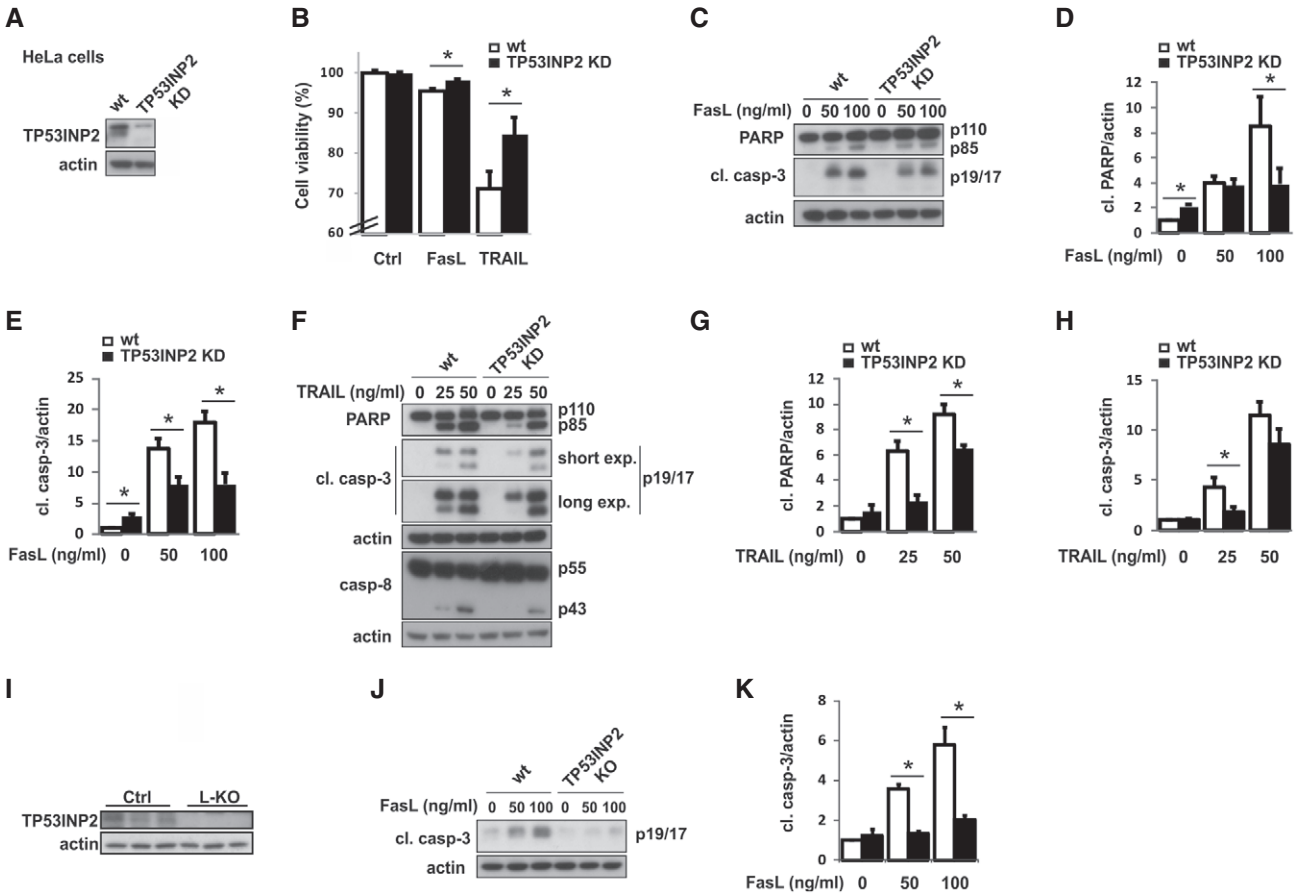

Figure 2. Loss of TP53INP2 renders cells resistant to death receptor-induced apoptosis.

A Western blot analysis of TP53INP2 in wild-type (wt) HeLa and TP53INP2 CRISPR KD cells.

B Cell viability of HeLa wt and TP53INP2 KD cells after 24 h treatment with FasL (50 ng/ml) or TRAIL (10 ng/ml) measured as annexin V- and PI-negative cells.

C HeLa control cells and TP53INP2 CRISPR KD cells were treated with different concentrations of FasL for 16 h, and cell lysates were subjected to Western blot analysis for PARP and caspase-3 cleavage.

D, E Quantification of protein levels of cleaved PARP (D) and cleaved caspase-3 (E) after FasL treatment.

F HeLa control cells and TP53INP2 CRISPR KD cells were treated with different concentrations of TRAIL for 4 h, and cell lysates were subjected to Western blot analysis for PARP1, caspase-3, and caspase-8 cleavage.

G, H Quantification of protein levels of cleaved PARP (G) and cleaved caspase-3 (H) after TRAIL treatment.

I Detection of TP53INP2 protein levels in livers of control and TP53INP2 L-KO mice.

J Control and TP53INP2 KO hepatocytes were treated with FasL for 16 h, and levels of cleaved caspase-3 were detected by Western blot.

K Quantification of protein levels of cleaved caspase-3 after FasL treatment.

Data information: Data are given as mean ± SEM and were analyzed by two-way Student's *t*-test; *n* = three independent experiments, $*P < 0.05$.
Source data are available online for this figure.

(Fig 2A–H). Thus, percentage of cell death was lower in TP53INP2-deficient cells compared to wild-type cells upon FasL or TRAIL (Fig 2B), and similarly, cleaved caspase-3 or PARP-1 was reduced in TP53INP2-deficient cells treated with FasL or TRAIL (Fig 2C–H).

Furthermore, we generated liver-specific TP53INP2 KO mice (L-KO) by crossing $Tp53inp2^{loxP/loxP}$ mice (Sala *et al*, 2014) with mice expressing Cre recombinase under the control of the albumin promoter. TP53INP2 protein levels were undetectable in livers of L-KO animals, and no changes in the protein levels in other tissues were detected (Fig 2I; Appendix Fig S2A and B). L-KO male and female mice showed normal body weight or blood glucose levels (Appendix Fig S2C and D). Primary hepatocytes isolated from these mice were less susceptible to FasL- and TNFα-induced apoptosis than hepatocytes from control mice (Fig 2J and K, and Appendix Fig S2E). Introducing TP53INP2 back to the L-KO hepatocytes by adenoviral infection restored the capacity of FasL or TNFα to induce apoptosis, as reflected by increased amounts of cleaved PARP-1 and cleaved caspase-3 (Appendix Fig S2E). Of note, overexpression of TP53INP2 *per se* in control and L-KO hepatocytes was pro-apoptotic (Appendix Fig S2E), thus making high amounts of TP53INP2 toxic for the liver.

Taken together, our results show that TP53INP2 increases susceptibility to death receptor-induced apoptosis and that it does so upstream of caspase activation, i.e., before TP53INP2 is cleaved by caspases.

Loss-of-function of TP53INP2 protects livers from FasL-induced apoptosis *in vivo*

We next tested whether TP53INP2 regulates death receptor-induced apoptosis *in vivo*. Control and L-KO mice were injected intraperitoneally with PBS or FasL for 4 h. The cleavage product of PARP-1 and cleaved caspase-3 were detected in controls, but were absent or present to a lesser extent in L-KO mice treated with FasL (Fig 3A and B). Of note, protein levels of p62 were increased and LC3II decreased in L-KO mice treated with PBS (Fig 3A), which is in keeping with prior observations in TP53INP2-deficient skeletal muscle (Sala *et al*, 2014). In addition, immunohistochemical staining showed more cleaved caspase-3 positive cells in control livers treated with FasL than in L-KO livers (Fig 3C and D). Analysis of TUNEL-positive cells further confirmed more apoptotic cells in control livers treated with FasL than in L-KO livers (Fig 3E and F). Given that caspase-8 activation is not sufficient to directly cleave caspase-3 in liver cells and the signal is amplified through mitochondria, we also checked by immunofluorescence the release of cytochrome c from mitochondria. TOM20 was used as marker of mitochondria. As expected, cytochrome c colocalized with TOM20 in PBS-treated livers of control and L-KO mice (Fig 3G and H; and Appendix Fig S3A). However, in FasL-treated livers of control animals, cytochrome c did not completely colocalize with this marker, indicating the release of cytochrome c from mitochondria (Fig 3G and H; and Appendix Fig S3A) and apoptosome formation, leading to the activation of executioner caspases (i.e., caspase-3). In contrast, colocalization of TOM20 and cytochrome c was detected in FasL-treated L-KO mice (Fig 3G and H, and Appendix Fig S3A).

To determine whether TP53INP2 deficiency has an impact on death receptor independent pathway, control and KD HeLa cells were treated with agents that induce intrinsic cell death such as doxorubicin, cisplatin, or actinomycin D. These agents reduced cell viability in a time-dependent manner (Fig 4A). However, only upon actinomycin D treatment, a significant increase in viability was detected in TP53INP2-deficient cells (Fig 4A). DEVDase activity was similarly induced in control and TP53INP2-deficient cells upon treatment with doxorubicin, cisplatin, or actinomycin D (Fig 4B), and cleaved PARP-1 was lower in TP53INP2 KD cells compared to controls upon cisplatin but not after doxorubicin and actinomycin D treatment (Fig 4D). Next, control and TP53INP2 L-KO mice were treated with doxorubicin or cisplatin for 48 h. No differences between control and L-KO groups were visualized when immunodetecting either cleaved caspase-3 (Fig 4E and F) or TUNEL-positive cells upon treatment with doxorubicin (Fig 4G and H). In contrast, cisplatin administration caused reduction in cleaved caspase-3 or TUNEL-positive cells in livers from L-KO mice compared with control mice (Fig 4E–H). Taken together, our data indicate that TP53INP2 regulates the cell death receptor pathway as well as some, but not all, of the intrinsic apoptotic pathways in mouse liver.

Regulation of death receptor signaling by TP53INP2 does not require canonical autophagy

Given that autophagy is involved in the regulation of caspase-8 activation (Bell *et al*, 2008; Pan *et al*, 2011; Huang *et al*, 2013), we first studied whether TP53INP2 sensitization to death receptor-induced apoptosis depends on autophagy. ATG5 was downregulated in HeLa cells by shRNA (Appendix Fig S4A), and apoptosis was induced with FasL. ATG5 deficiency did not abrogate DEVDase activity and apoptosis (Appendix Fig S4B), thereby indicating that canonical autophagy does not participate in the mechanism by which TP53INP2 sensitizes cells to FasL-induced apoptosis. We further confirmed this observation by generating ATG7 KO cells with CRISPR technology, and we obtained the same results as with the ATG5 KD model (Appendix Fig S4C–G). In addition, inhibition of autophagy with bafilomycin A1 (Baf A1) or wortmannin (Wort) did not rescue the enhanced FasL-induced apoptosis in TP53INP2-expressing cells (Appendix Fig S4H). All together, these data show that TP53INP2 sensitization to FasL does not require autophagy or intracellular DISC formation.

TP53INP2 interacts with and increases the levels of ubiquitinated caspase-8

An autophagy cargo protein, p62, has been shown to directly activate caspase-8 by aggregating ubiquitinated caspase-8 (Jin *et al*, 2009). TP53INP2 overexpression upregulates p62 (Sala *et al*, 2014); thus, we addressed whether TP53INP2 function in death receptor signaling is dependent on p62. The downregulation of p62 did not rescue FasL-induced cell death in TP53INP2-expressing cells, even though there was slightly less apoptosis in p62 knock-down cells (Appendix Fig S4I and J). On the basis of these observations, we then explored whether TP53INP2 participates directly in caspase-8 activation. Caspase-8-deficient cells (Appendix Fig S4K) showed reduced FasL-induced apoptosis in control and TP53INP2-expressing cells (Appendix Fig S4L and M). Surprisingly, caspase-8 knock-down cells tolerated higher protein levels of TP53INP2 than the scrambled cells (Appendix Fig S4M), thereby further corroborating our hypothesis that TP53INP2 acts directly through caspase-8. In order to prove this, we examined whether TP53INP2 aggregated caspase-8 in a similar way as p62, especially since both proteins bind ubiquitin and are aggregation-prone. TP53INP2 aggregated caspase-8 to almost the same extent as p62 (Fig 5A and B); however, caspase-8 dots in TP53INP2-overexpressing cells were much smaller than those in p62-overexpressing ones. These observations suggest that p62 has higher affinity to ubiquitinated caspase-8 than TP53INP2 and/or that TP53INP2 acts upstream of the aggregation of ubiquitinated caspase-8. To confirm that TP53INP2 has a direct effect on caspase-8 activation, we next examined whether the two proteins colocalize. Caspase-8 and TP53INP2 colocalized in a dot-like manner, but again to a lesser extent than p62 (Appendix Fig S4N). Since we previously showed that TP53INP2 dislocates p62 from LC3 in autophagy (Sala *et al*, 2014), a process in which the two proteins compete for the same binding site, we examined whether they also compete for the same binding sites in caspase-8 or ubiquitinated caspase-8. To test this notion, we co-expressed p62, TP53INP2, and caspase-8 and analyzed their localization. All three proteins colocalized in large aggregate-like dots (Appendix Fig S4O), thereby suggesting that they are in the same pathway and that p62 and TP53INP2 do not exclude each other from caspase-8-positive dots; i.e., TP53INP2 and p62 do not bind to the same binding sites in (ubiquitinated) caspase-8. We confirmed this also with endogenous proteins in Snu449 cells, in which TP53INP2, p62, and caspase-8 completely colocalized when caspase-8 was aggregated upon TRAIL treatment (Fig 5C and D).

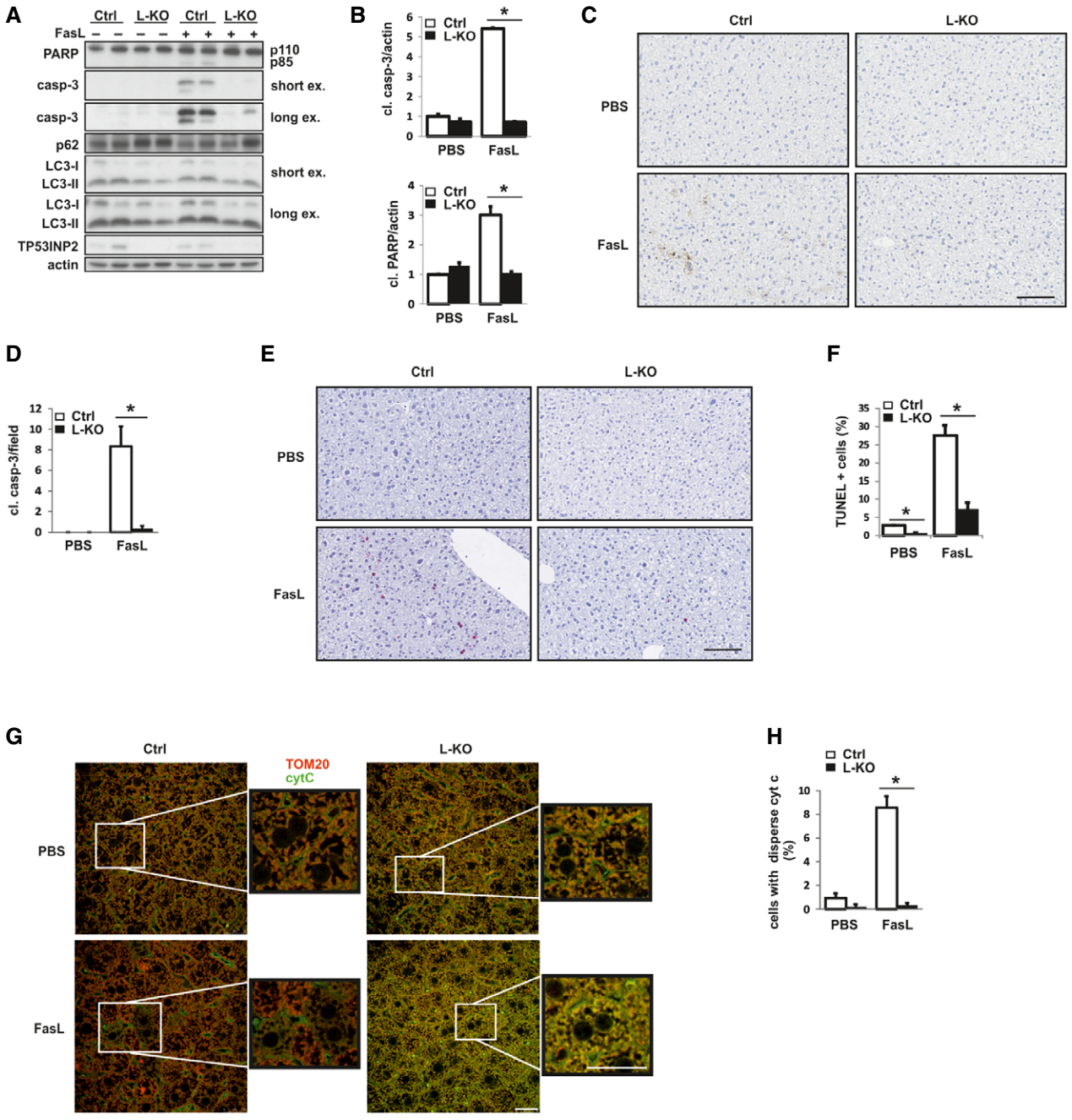

Figure 3. TP53INP2 deficiency protects livers from FasL-induced apoptosis.

A Control and TP53INP2 L-KO animals were injected with PBS or FasL i.p. for 4 h. Whole liver lysates were subjected to immunodetection of the indicated apoptotic and autophagic markers.

B Quantification of Western blot of cleaved caspase-3 and PARP. Data are presented as mean ± SEM of four samples.

C Cleaved caspase-3 immunohistochemistry staining of livers from control and TP53INP2 L-KO mice treated with PBS or FasL (Scale bar, 100 μm).

D Quantification of cleaved caspase-3 immunohistochemistry staining. Data are presented as mean ± SEM of nine different fields (per mice) where in each field more than 200 cells were counted.

E TUNEL immunohistochemistry staining of livers from control and TP53INP2 L-KO mice treated with PBS or FasL (Scale bar, 100 μm).

F Quantification of TUNEL immunohistochemistry staining. Data are presented as mean ± SEM of more than 1,500 cells counted per mice (four mice in each experimental group).

G TOM20 (red) and cytochrome C (green) immunohistofluorescence staining of livers from control and TP53INP2 L-KO mice (Scale bar, 25 μm).

H Quantification of cells with disperse cytochrome *c* staining. Data are presented as mean ± SEM of more than 300 cells counted per each experimental group.

Data information: Two-way Student's *t*-test was performed, $*P < 0.05$.
Source data are available online for this figure.

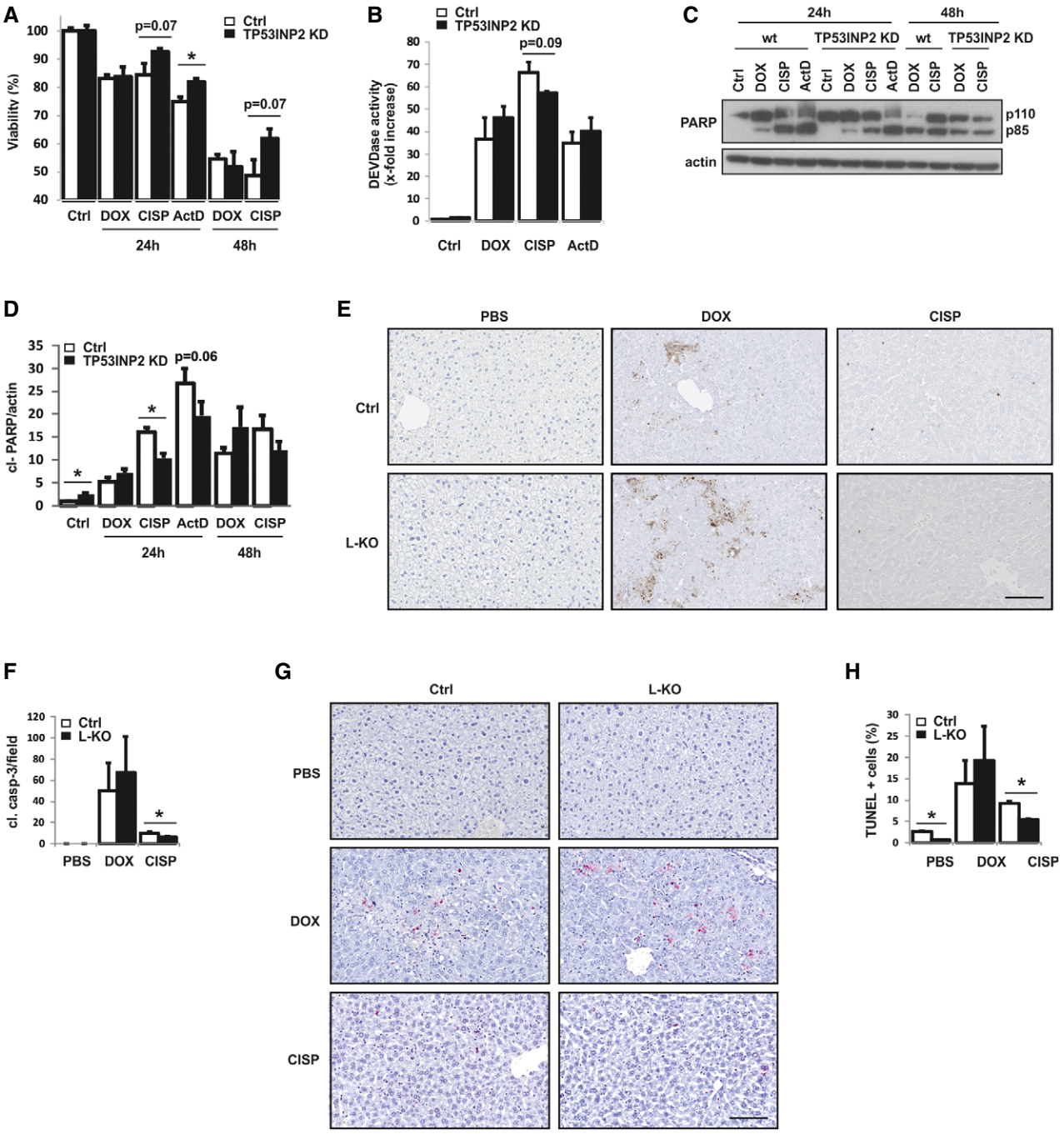

Figure 4. TP53INP2 differentially sensitizes to intrinsic apoptotic inducers.

A, B Viability (A) and DEVDase activity (B) of HeLa control and TP53INP2 KD cells treated with doxorubicin, cisplatin, and actinomycin D. Data are presented as mean ± SEM of n = 4–8 of independent experiments in (A) and three in (B).

C Immunodetection of cleaved PARP in control and TP53INP2 KD cells after treatment with doxorubicin, cisplatin, and actinomycin D.

D Quantification of protein levels of cleaved PARP. Data are presented as mean ± SEM of at least three independent experiments.

E Cleaved caspase-3 immunohistochemistry staining of livers from control and TP53INP2 L-KO mice treated with PBS, doxorubicin, or cisplatin (Scale bar, 100 μm).

F Quantification of cleaved caspase-3 immunohistochemistry staining. Data are presented as mean ± SEM of nine different fields (per mice) where in each field more than 200 cells were counted.

G TUNEL immunohistochemistry staining of livers from control and TP53INP2 L-KO mice treated with PBS, doxorubicin, or cisplatin (Scale bar, 100 μm).

H Quantification of TUNEL immunohistochemistry staining. Data are presented as mean ± SEM of more than 1,500 cells counted per mice (four mice in each experimental group).

Data information: Two-way Student's t-test was performed, $^*P < 0.05$.
Source data are available online for this figure.

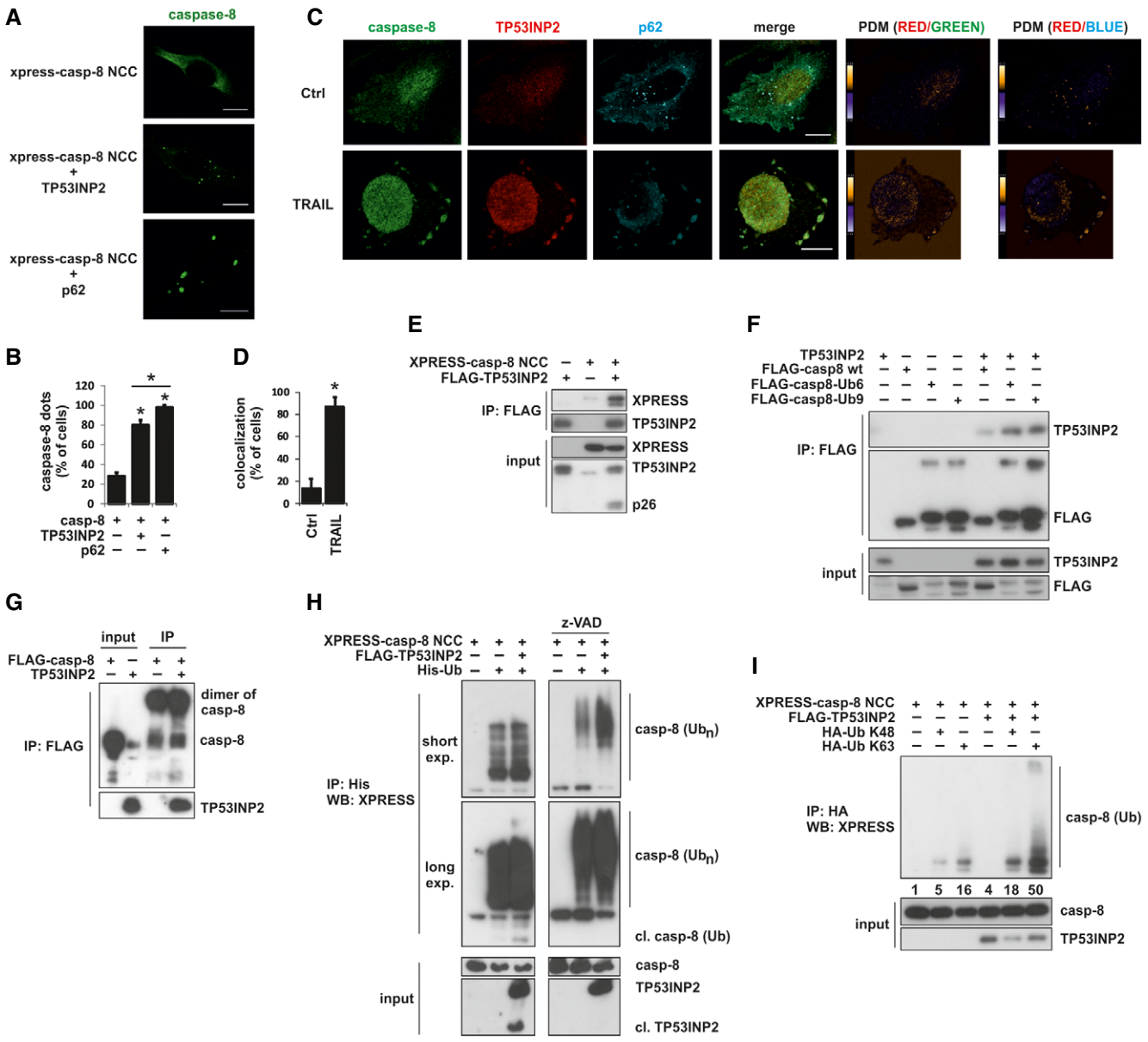

Figure 5. TP53INP2 interacts with caspase-8 and regulates its ubiquitination levels.

A HeLa cells were transfected with xpress-casp-8-NCC alone or together with TP53INP2 or p62. Caspase-8 in dimers/aggregating localization and dot-like structures were detected with xpress antibody (Scale bar, 10 μm).

B Quantification of caspase-8 dots in immunofluorescence experiment. Data are presented as mean ± SEM of 25 cells per experimental group.

C Immunofluorescence colocalization analysis of caspase-8 with TP53INP2 and p62 in Snu449 cells in control or TRAIL (250 ng/ml) treated cells for 30 min (Scale bars, 10 μm).

D Quantification of the colocalization. Data are presented as mean ± SEM of 25 cells per experimental group.

E HEK293T cells were transfected with xpress-casp-8-NCC and FLAG-TP53INP2, and 24 h later, cell lysates were pulled down with FLAG resin. IPs and inputs were afterward immunodetected with xpress and TP53INP2 antibody.

F HEK293T cells were transfected with wt FLAG-casp-8 or FLAG-casp-8-Ub6 or FLAG-casp-8-Ub9 with or without TP53INP2 in the presence of 20 μM z-VAD-fmk. Pull-down assays were done with FLAG resin. IPs and inputs were immunodetected with FLAG or TP53INP2 antibodies.

G Pull-down assay of recombinant pro-caspase-8 and TP53INP2.

H HEK293T cells were transfected with xpress-casp-8-NCC, His-Ub, and TP53INP2 in the presence or absence of 20 μM z-VAD-fmk. Denaturing pull-down assays were done with His resin. IPs and inputs were immunodetected with the indicated antibodies.

I Denaturing pull-down assays of HEK293T cells transfected with indicated plasmids. IPs and inputs were subjected to immunodetection with xpress, casp-8, and TP53INP2 antibodies. The amount of ubiquitinated casp-8 was quantified with Fiji software.

Data information: Two-way Student's *t*-test was performed, $*P < 0.05$.
Source data are available online for this figure.

Surprisingly, TP53INP2 is not mainly nuclear in Snu449 cells (Fig 5C). This is coherent with the fact that caspase-8 activation in death receptor-induced apoptosis is cytosolic. We further analyzed whether the cellular localization of TP53INP2 in HeLa cells is coherent with the cytosolic aggregation and activation of caspase-8. Immunolocalization and subcellular fractionation assays revealed that TP53INP2 was mainly nuclear in HeLa cells at all times after TRAIL treatment, but a significant proportion of TP53INP2 was also cytosolic, and therefore available for interaction with caspase-8 (Appendix Fig S5A–D, Movie EV1).

In order to further confirm the interaction, we performed co-immunoprecipitation experiments of caspase-8 and TP53INP2. We pulled down caspase-8 with TP53INP2 (Fig 5E), and this interaction was not due to the ubiquitination of TP53INP2, since we obtained the same result with a TP53INP2 mutant that cannot be ubiquitinated (3KR, Appendix Fig S4P). Moreover, we pulled down TP53INP2 with wild-type caspase-8 and to a higher extent with chimeric proteins of caspase-8 fused to 6 or 9 ubiquitins (Fig 5F). In this experiment, we added z-VAD-fmk to the cells due to high levels of apoptosis, especially in those transfected with caspase-8-Ub6 or caspase-8-Ub9. Altogether, our pull-down assays showed that TP53INP2 and caspase-8 interact and that this interaction is stronger in the presence of ubiquitin(s). We can rule out this interaction being due exclusively to the cleavage of TP53INP2 by caspase-8 since we also detected it in the presence of z-VAD-fmk, an inhibitor of caspases that irreversibly binds to the catalytic site of caspase proteases.

Our results indicate that TP53INP2 binds to caspase-8 and/or ubiquitinated caspase-8. To discriminate between these two possibilities, we tried to identify the ubiquitin-binding motifs in TP53INP2. We split TP53INP2 into two halves and used these constructs for the pull-down assays. The N-terminal half of TP53INP2 retained capacity to interact with ubiquitin/ubiquitinated proteins, while interaction with the C-terminal half was almost completely abolished (Appendix Fig S6A). We excluded the possibility of the N-terminal part being ubiquitinated as all three Lys residues in the protein are at the C-terminal. We checked the TP53INP2 sequence and identified a potential ubiquitin-interacting motif (UIM; Appendix Fig S6B). Mutation of the key residues in the UIM motif (Appendix Fig S4B) caused a 20% decrease in the interaction of TP53INP2 ALA mutant with ubiquitin (Appendix Fig S6C and D). This observation suggests that besides the potential UIM motif TP53INP2 has additional ubiquitin-binding motifs/domains. Since we could not make a mutant of TP53INP2 lacking the capacity to bind ubiquitin, we performed experiments with recombinant proteins. As seen in Fig 5G, we pulled down TP53INP2 with caspase-8 in the absence of ubiquitin (even when caspase-8 was aggregating), supporting the view that TP53INP2 interacts directly with caspase-8.

We next tested whether TP53INP2 acts upstream of caspase-8 ubiquitination, i.e., whether it participates in the regulation of caspase-8 ubiquitination. We performed denaturing pull-down assays with His-Ub and caspase-8 in the presence or absence of TP53INP2. The addition of TP53INP2 upregulated the levels of ubiquitinated caspase-8, and caspase-8 and TP53INP2 were cleaved, thereby confirming faster activation of caspase-8 in the presence of TP53INP2 (Fig 5H). In order to fully appreciate the difference in the degree of caspase-8 ubiquitination, experiments were performed by pre-treating the cells with z-VAD-fmk. Again, and to a much higher extent, TP53INP2 upregulated the levels of ubiquitinated caspase-8 compared with the sample without TP53INP2 (Fig 5H). Several studies have reported that ubiquitin chains added to caspase-8 can be K48 or K63 (He *et al*, 2006; Jin *et al*, 2009; Gonzalvez *et al*, 2012; Li *et al*, 2013). Ubiquitin K48 chains mark caspase-8 for degradation, while ubiquitin K63 can enhance or block the activation of the caspase-8, depending on which Lys residue is ubiquitinated. To determine the chains that are preferentially added to caspase-8 in the presence of TP53INP2, we used mutants of ubiquitin that can make only K48 or K63 chains. As expected, mainly because TP53INP2 enhances apoptosis, we detected an increase in the K63 ubiquitination of caspase-8 in the presence of TP53INP2 (Fig 5I), precisely the type of ubiquitination that favors caspase-8 activation. Collectively, our data show that TP53INP2 colocalizes and interacts with caspase-8. Moreover, they reveal that TP53INP2 promotes caspase-8 ubiquitination with K63 ubiquitin chains.

TP53INP2 sensitization to death receptor-induced apoptosis is dependent on TRAF6

TP53INP2 is not an E3 ubiquitin ligase, but it may act as a scaffold, bringing together several components of the same complex for a more efficient function of the signaling hub. To determine the E3 ubiquitin ligase responsible for the enhanced ubiquitination of caspase-8 in the presence of TP53INP2, we first analyzed cullin-3, which ubiquitinates caspase-8 with K63 chains in death receptor-induced apoptosis (Jin *et al*, 2009). We did not detect any interaction between TP53INP2 and cullin-3 (Appendix Fig S7A). Furthermore, we repressed cullin-3 expression (Appendix Fig S7B) and induced apoptosis with FasL in control and TP53INP2-expressing cells. No differences in the levels of cleaved caspase-3 were detected in wild-type or CUL3-deficient cells upon TP53INP2 expression (Appendix Fig S7C). These observations thus exclude this E3 ubiquitin ligase as being responsible for enhanced caspase-8 ubiquitination in the presence of TP53INP2.

Two more E3 ubiquitin ligases, TRAF6 and HECTD3, have been reported to add K63 chains to caspase-8 during death receptor-induced apoptosis (He *et al*, 2006; Li *et al*, 2013). HECTD3 K63-linked polyubiquitination of caspase-8 inhibits its activation, so we focused on TRAF6. TRAF6 was knocked out by CRISPR technology (Fig 6A). The absence of TRAF6 alone decreased FasL- and TRAIL-induced apoptotic cell death compared to control cells (Fig 6A). The same was seen in MDA231 TRAF6 KO cells (Appendix Fig S8A). In addition, TRAF6 deficiency reduced FasL- and TRAIL-induced caspase activity, the levels of cleaved caspase-3 and cleaved PARP-1, and percentage of cell death in TP53INP2-expressing cells (Fig 6B–H, and Appendix Fig S8B). Furthermore, we obtained similar results in TRAF6 KO MEF cells (Appendix Fig S8C and D).

Moreover, TP53INP2 immunoprecipitated with TRAF6 in basal conditions and to a greater extent after a 20 min treatment of the cells with FasL (Fig 6I). However, this interaction appeared to be transient, since the amount of TP53INP2 immunoprecipitated dropped after 1 h of FasL treatment, or, on the other hand, caspase-8 was already activated in TRAF6- and TP53INP2-overexpressing cells and started cleaving TP53INP2, which might explain the decrease in the levels of TP53INP2 in the extracts (inputs in Fig 6I). In addition, the interaction of TRAF6 and TP53INP2 did not depend

on the ubiquitination of TP53INP2 by TRAF6, since the TP53INP2 3KR mutant interacted with TRAF6 to same extent (Appendix Fig S8E).

We mapped a TRAF6-interacting motif (TIM; Ye *et al*, 2002) in the N-terminal part of TP53INP2 (Fig 6J). We mutated the two key residues in the TIM, generating the TP53INP2 TIM mutant (Fig 6J).

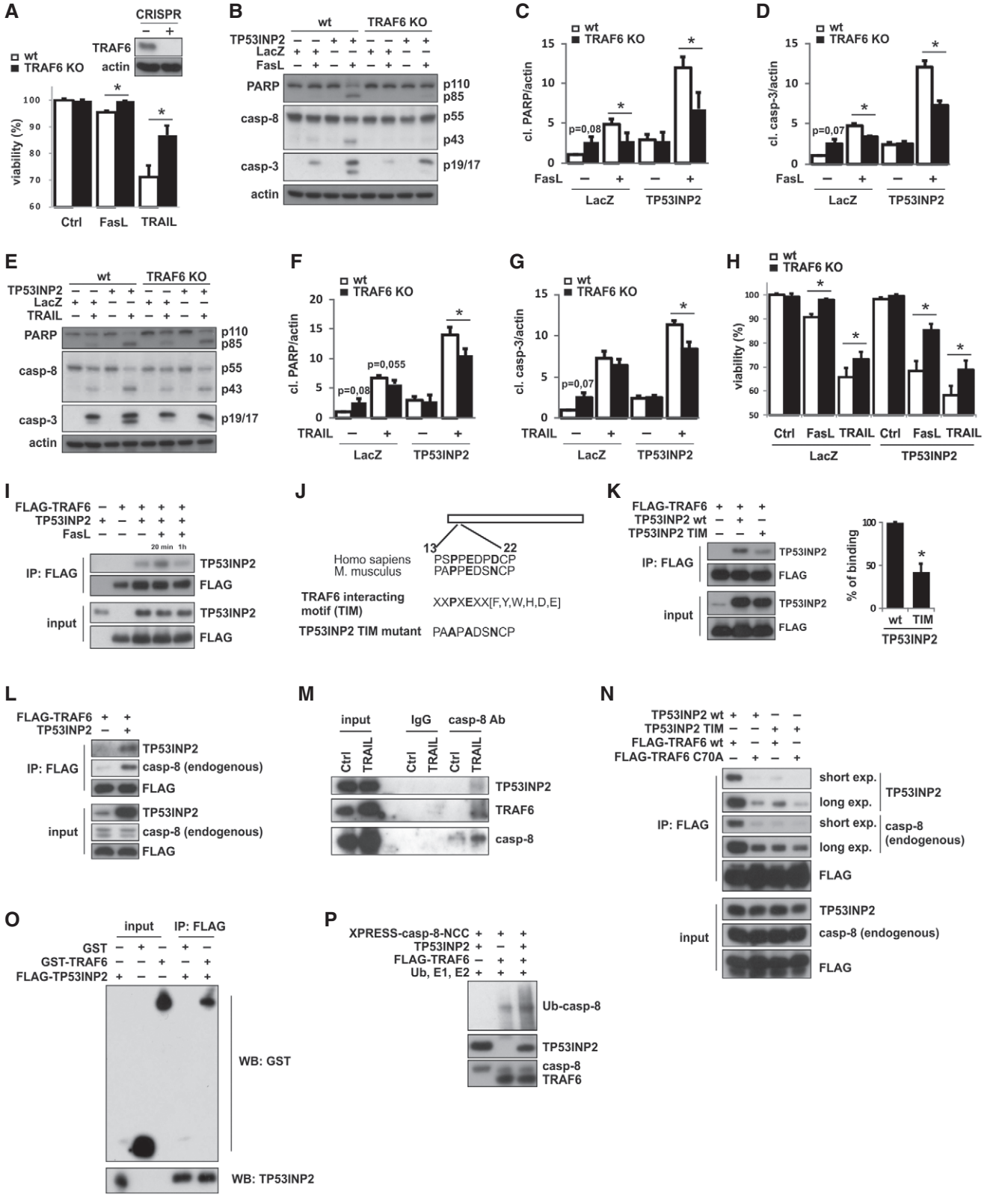

Figure 6.

Figure 6. TRAF6 is indispensable for TP53INP2 function in death receptor-induced apoptosis.

A Western blot analysis of TRAF6 and viability assay in wt HeLa cells and TRAF6 CRISPR KO cells. Data are presented as mean ± SEM of five independent experiments.

B HeLa wt and TRAF6 KO cells expressing LacZ or TP53INP2 were treated with 50 ng/ml FasL for 16 h, and whole lysates were analyzed by Western blot against PARP-1, caspase-8, and caspase-3 antibodies.

C, D Quantification of protein levels of cleaved PARP and caspase-3. Data are presented as mean ± SEM of three independent experiments.

E HeLa wt and TRAF6 KO cells expressing LacZ or TP53INP2 were treated with 25 ng/ml TRAIL for 4 h, and whole lysates were analyzed by Western blot against PARP-1, caspase-8, and caspase-3 antibodies.

F, G Quantification of protein levels of cleaved PARP and caspase-3. Data are presented as mean ± SEM of three independent experiments.

H Viability assay of HeLa wt and TRAF6 KO cells expressing LacZ or TP53INP2 and treated with 50 ng/ml FasL or 10 ng/ml TRAIL for 24 h. Data are presented as mean ± SEM of five to eight independent experiments.

I HEK293T cells expressing FLAG-TRAF6 and/or TP53INP2 were left untreated or treated with FasL (100 ng/ml) for the indicated times and then immunoprecipitated with FLAG resin. Immunocomplexes were subjected to Western blot analysis with anti-FLAG and anti-TP53INP2 antibodies.

J Schematic presentation of the consensus TRAF6 interaction motif (TIM) in TP53INP2 protein and the amino acids mutated in a TP53INP2 TIM mutant.

K HEK293T cells expressing FLAG-TRAF6, wt TP53INP2, and TIM mutant were immunoprecipitated with FLAG resin, and immunocomplexes were analyzed by Western blot with anti-FLAG and anti-TP53INP2 antibody. The amount of TP53INP2 precipitated with TRAF6 was quantified with Fiji software. Data are presented as mean ± SEM of three independent experiments.

L HEK293T cells expressing FLAG-TRAF6 and TP53INP2 were immunoprecipitated with FLAG resin, and immunocomplexes were subjected to Western blot analysis with anti-FLAG, anti-TP53INP2, and anti-caspase-8 antibody. Note that we were able to immunoprecipitate endogenous caspase-8 in the same complex with TRAF6 and TP53INP2.

M HeLa cells stably overexpressing TP53INP2 were left untreated or treated with 100 ng/ml TRAIL for 30 min and subjected to immunoprecipitation with caspase-8 antibody. Immunocomplexes were subjected to Western blot analysis with anti-TRAF6, anti-TP53INP2, and anti-caspase-8 antibody.

N The same as in (L), except that we also expressed FLAG-TRAF6 C70A and/or TP53INP3 TIM mutant.

O Pull-down assay of recombinant GST-TRAF6 and FLAG-TP53INP2 proteins using FLAG resin and Western blot analysis of immunocomplexes with anti-GST and anti-TP53INP2 antibodies.

P *In vitro* ubiquitination assay with immunoprecipitated xpress-casp-8-NCC, FLAG-TRAF6, and TP53INP2.

Data information: Two-way Student's *t*-test was performed, $*P < 0.05$.
Source data are available online for this figure.

The mutation of TIM in TP53INP2 reduced the binding to TRAF6 by about 50% compared to the wild type (Fig 6K). Mutations of TP53INP2 in the N-terminal might alter its exit from the nucleus; however, we proved that this was not the case with the TIM mutant, in contrast to the LIR mutant, which was unable to leave the nucleus (Appendix Fig S8F). Moreover, overexpression of the TIM and LIR mutant decreased the levels of FasL-induced apoptosis compared to the wild-type TP53INP2 (Appendix Fig S8G), thereby suggesting that the sensitization of TP53INP2 to FasL apoptosis relies on its binding to TRAF6 and also on its ability to exit the nucleus. In addition, we co-immunoprecipitated endogenous caspase-8 with TRAF6. The interaction was stronger in the presence of TP53INP2 (Fig 6L), thus indicating that caspase-8, TRAF6, and TP53INP2 are in the same complex. We could also co-immunoprecipitate endogenous TRAF6 and TP53INP2 with endogenous caspase-8 in HeLa cells stably expressing TP53INP2 (Fig 6M). Catalytically inactive TRAF6 (C70A) did not pull down the endogenous caspase-8. Also, the amount of TP53INP2 was reduced dramatically (Fig 6N), implying that the strength of the caspase-8/TRAF6/TP53INP2 complex depends on the ubiquitination activity of TRAF6. Since the TP53INP2 TIM mutant and the TRAF6 C70A mutant reduced the binding of TRAF6 and TP53INP2 to the same extent, we speculated that the remaining binding between the two proteins (in Fig 6N) is not due to an additional TRAF6 binding site in TP53INP2 but to the binding of TP53INP2 to ubiquitinated TRAF6 itself or to other ubiquitinated components of the complex. Indeed, expression of the TP53INP2 TIM and TRAF6 C70A mutants abolished the interaction between the two proteins (Fig 6N). The direct interaction between the two proteins (TRAF6 and TP53INP2) was also seen in *in vitro* pull-down of recombinant proteins (Fig 6O). To confirm that TP53INP2 upregulates caspase-8 ubiquitination in the presence of TRAF6, we performed an *in vitro* ubiquitination assay. TRAF6 alone ubiquitinated caspase-8. However, the addition of TP53INP2 further increased the ubiquitination of caspase-8 (Fig 6P).

Taken together, our results support the notion that TP53INP2 acts as a scaffold for caspase-8 ubiquitination by TRAF6.

Protein levels of TP53INP2 correlate with sensitivity of cancer cell lines to TRAIL treatment

TRAIL kills cancer cells selectively without major damage to normal cells. Therefore, this specific apoptotic pathway has been extensively studied for possible clinical applications (Naoum *et al*, 2017). However, initial enthusiasm was back-fired by unsuccessful TRAIL pre-clinical/clinical trials that highlighted the need for optimized TRAIL antagonists and for strategies to optimize the selection of patients who would most benefit from TRAIL treatment (i.e., through biomarkers; de Miguel *et al*, 2016; Naoum *et al*, 2017; von Karstedt *et al*, 2017). In line with this notion, our results suggest that TP53INP2 may serve as a potential biomarker for the selection of patients for TRAIL treatment. In order to further explore this possibility, we first screened several breast cancer cell lines for protein levels of TP53INP2 and then determined the percentage of cells undergoing apoptosis upon TRAIL treatment. The cell lines differed in their protein levels of TP53INP2: those with highest levels were BT20, whereas MCF7 and BT474 showed no TP53INP2 or undetectable levels (Fig 7A). As expected, BT20 cells were the most sensitive to TRAIL treatment, whereas the cell lines with no or less TP53INP2 did not undergo apoptosis (Fig 7B, and Appendix Fig S9A and C). Moreover, there was a positive correlation ($r = 0.84$) between the protein levels of TP53INP2 and susceptibility to apoptosis (Fig 7C). We did the same set of experiments in various liver cancer cell lines and obtained the same results; i.e., Snu449 cells had the highest levels of TP53INP2 and responded to TRAIL

treatment, while those with no or almost undetectable levels of TP53INP2 did not (Fig 7D and E; Appendix Fig S9B and D). In the case of liver cancer cell lines, we also detected a positive correlation between TP53INP2 and percentage of dying cells ($r = 0.87$; Fig 7F). The expression of Bcl-2 homologues did not correlate with TP53INP2 expression in the different cells studied (Appendix Fig S9E and F). In addition, the differences observed in the Bcl-2 homologues between different cell lines do not explain the differences seen in susceptibility to TRAIL treatment (Appendix Fig S9E and F). Moreover, downregulation of TP53INP2 expression in MDA231 and Snu449 cells reduced the response to TRAIL treatment (Fig 7G–J). On the contrary, the overexpression of TP53INP2 in different breast and liver cancer cell lines with no or low levels of TP53INP2 sensitized them to TRAIL-induced apoptosis (Appendix Fig S9G–J).

Collectively, our results suggest that cancer cell lines that express high levels of TP53INP2 will respond favorably to TRAIL-induced apoptosis and that TP53INP2 might be a good biomarker of responsiveness to TRAIL treatment.

Discussion

The engagement of death ligands with death receptors can trigger three signaling cascades, i.e., apoptosis, necroptosis, or the NF-kB pathway (Tummers & Green, 2017), depending on the signaling complexes being formed downstream of death receptors and the proteins expressed in a given cell. Recently, several new components in this pathway have been reported (Jin *et al*, 2009; Murphy *et al*, 2013; Lu *et al*, 2014; de Miguel *et al*, 2016), thus increasing their complexity and shedding light on how the same event can give such divergent outcomes. In the context of cancer, it is important to understand how we can manipulate the death receptor pathway and switch between outcomes, in this case preferentially to apoptosis. Here, we have shown that TP53INP2 is one of such switches, favoring apoptosis in cells that have a sufficient amount of TP53INP2. Increasing the amount of TP53INP2 in cells depleted or deficient in this protein by adenoviral or other means of manipulating its expression would sensitize them to TRAIL. It is important to state that TP53INP2 exerts this role in cells where active caspase-8 can induce apoptosis. In cells with low caspase-8 expression, the apoptotic effect of TP53INP2 is reduced. Surprisingly, in caspase-8 knock-down cells, the protein levels of TP53INP2 tolerated are much higher than in wild-type cells, thus suggesting that caspase-8 regulates TP53INP2 protein levels or that cells with a high amount of both caspase-8 and TP53INP2 undergo apoptosis spontaneously. Indeed, we observed spontaneous apoptosis of TP53INP2-overexpressing primary hepatocytes. This finding would indicate that high protein levels of TP53INP2 are toxic.

TP53INP2 is an intrinsically disordered protein, which makes difficult any prediction of protein-protein interactions. However, it is a scaffold, thus explaining its role in mediating protein-protein interactions, most probably through short binding motifs like in the case of LIR (LC3 interacting region; Sancho *et al*, 2012) or hormone nuclear binding motif (Baumgartner *et al*, 2007), which are just few amino acids long and are sufficient for efficient interaction and scaffolding function in signaling hubs. Here, we identified a TIM (Ye *et al*, 2002) around 20 amino acids preceding LIR motif in TP53INP2. The binding of TRAF6 would probably sterically impede the interaction with LC3 at the same time, thus explaining why we do not see a major effect of autophagy on TP53INP2 sensitization to death receptor signaling. In contrast, we were unable to identify all the ubiquitin binding sites in TP53INP2. Since TP53INP2 is an acidic protein, additional binding to ubiquitin in the TP53INP UIM mutant might be due to the interaction of negatively charged amino acids of TP53INP2 with positively charged surface patches in ubiquitin, thereby accommodating the secondary structure of TP53INP2 upon binding, a phenomenon known to occur when intrinsically disordered proteins bind to their cognitive interactors.

Our data demonstrate that TP53INP2 activates caspase-8 by promoting its ubiquitination by TRAF6 and, in consequence, it shifts the response toward apoptotic cell death. TP53INP2 acts as a signaling adaptor, bringing together crucial components of the signaling pathway, namely TRAF6, caspase-8, and ubiquitin (Fig 8A–C). The TIM of TP53INP2 is postulated to bind to the canonical adaptor binding groove of the TRAF_C domain of TRAF6, a domain that normally recognizes upstream regulators of TRAF6 (Ye *et al*, 2002; Shi *et al*, 2015). The N-terminal RING finger domain of TRAF6 binds to the E2 Ubc13 displaying E3 ubiquitin ligase activity and mediating K63-linked ubiquitination of caspase-8, thus modulating activation of apoptosis (Fig 8B and C; Wooff *et al*, 2004). We propose that TP53INP2, like p62, binds to ubiquitinated caspase-8, probably before the caspase is fully activated. Activated caspase-8 can cleave TP53INP2 at the LIR motif, thus separating the part encompassing the TIM from the rest of the protein, including the UIM region. This cleavage would inactivate TP53INP2 function in death receptor-induced apoptosis, but also in autophagy, since it cuts off the LIR region from the major part of the protein. In contrast to our previous data on autophagy, where TP53INP2 and p62 are mutually exclusive in binding to Atg8 homologues (Sala *et al*, 2014), both can bind to ubiquitinated caspase-8 and promote its activation. In addition, p62 also binds to TRAF6 and, like TP53INP2, participates in determining TRAF6 substrates (Jadhav *et al*, 2011). It will be interesting to determine the extent to which the substrates are shared between the TRAF6/p62 and TRAF6/TP53INP2 complexes and to identify those that are unique to each complex. Caspase-8 may not be common to the two scaffold proteins, since it does not have the TRAF6/p62 ubiquitination consensus site (Jadhav *et al*, 2011), and repression of p62 does not rescue TP53INP2 sensitization to death receptor-induced apoptosis (Appendix Fig S3F and G). Our data, in addition to other studies (Jin *et al*, 2009), indicate that p62 interacts with ubiquitinated caspase-8 and facilitates its aggregation and full activation. Since both p62 and TP53INP2 are involved in differentiation (Linares *et al*, 2011; McManus & Roux, 2012; Li *et al*, 2014; Sugiyama *et al*, 2017), apoptosis (Jin *et al*, 2009; Moscat & Diaz-Meco, 2009; Bhattacharya *et al*, 2015), nuclear hormone receptor signaling (Baumgartner *et al*, 2007; Duran *et al*, 2016), diabetes (Sala *et al*, 2014; Kruse *et al*, 2015; Long *et al*, 2017), and autophagy (Pankiv *et al*, 2007; Moscat & Diaz-Meco, 2009; Nowak *et al*, 2009; Mauvezin *et al*, 2010; Sancho *et al*, 2012), further studies are needed to unravel how they interplay/overlap in these pathways. Along the same line, TRAF6 has been implicated in multiple signaling pathways, such as autophagy, development, and immunity (Linares *et al*, 2015; Walsh *et al*, 2015). We previously showed that TP53INP2 modulates skeletal muscle mass by regulating autophagy (Sala *et al*, 2014), and the same has been shown for TRAF6 (Paul & Kumar, 2011). These observations thus suggest that these two

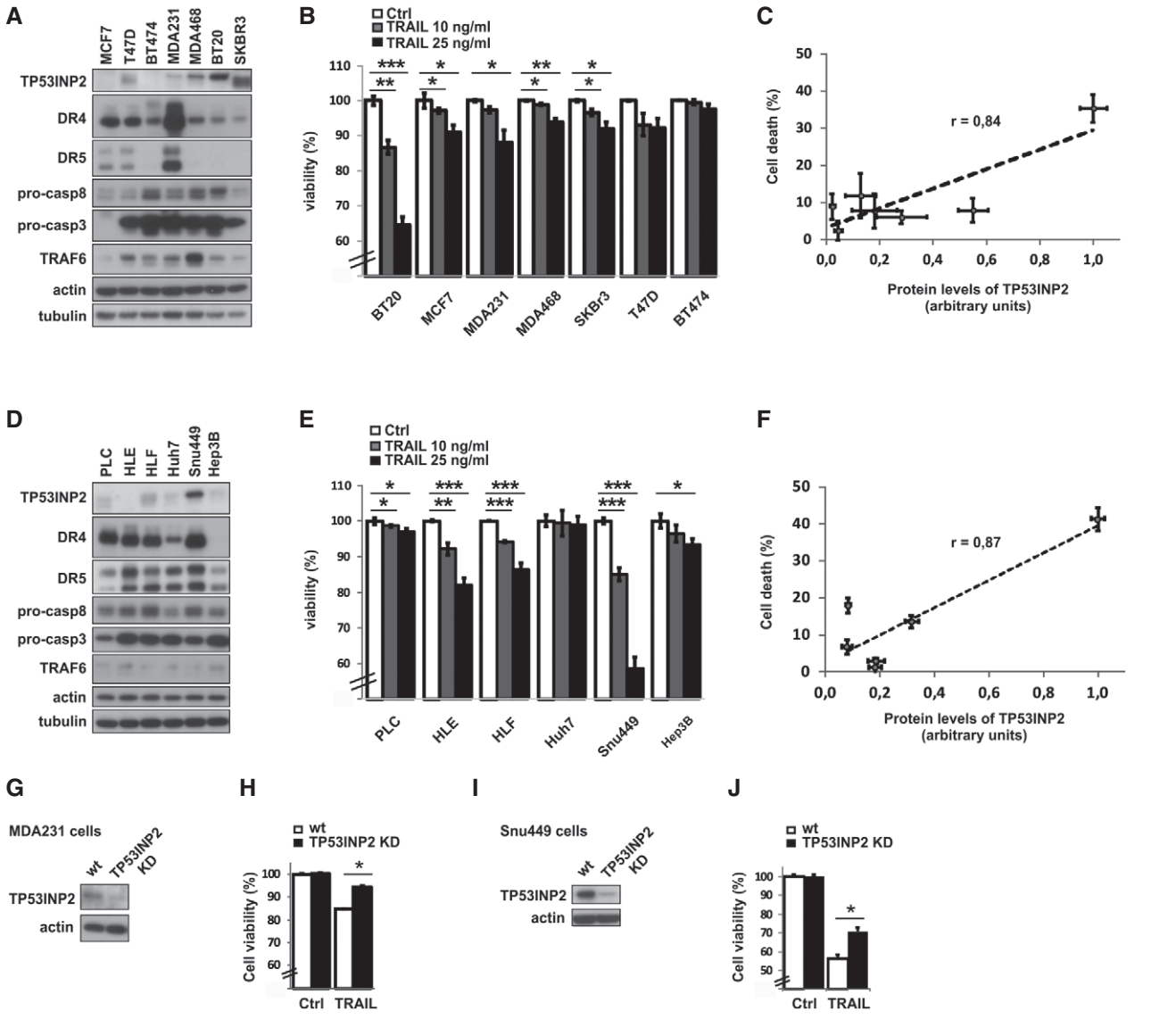

Figure 7. TP53INP2 is a molecular biomarker for TRAIL responsive tumor cell lines.

A Set of breast cancer cell lines analyzed by Western blot for the protein levels of TP53INP2 and other components of the TRAIL signaling pathway.

B Viability of breast cancer cell lines after 24 h with 10 or 25 ng/ml of TRAIL was measured by annexin V and PI using flow cytometer. Cells that were annexin V- and PI-negative were considered viable. Data are presented as mean ± SEM of three independent experiments.

C Correlation plot of TP53INP2 protein levels and cell death in breast cancer cell lines; *r* = Pearson's coefficient.

D Set of liver cancer cell lines analyzed by Western blot for the protein levels of TP53INP2 and other components of the TRAIL signaling pathway.

E Viability of liver cancer cell lines after 24 h with 10 or 25 ng/ml of TRAIL was measured by annexin V and PI using a flow cytometer. Cells that were annexin V- and PI-negative were considered viable. Data are presented as mean ± SEM of three or four independent experiments.

F Correlation plot of TP53INP2 protein levels and cell death in liver cancer cell lines; *r* = Pearson's coefficient.

G Western blot of TP53INP2 in MDA231 wt and CRISPR KD cells.

H Cell viability of MDA231 wt and TP53INP2 KD cells after 25 ng/ml TRAIL treatment. Data are presented as mean ± SEM of three or four independent experiments.

I Western blot of TP53INP2 in Snu449 wt and CRISPR KD cells.

J Cell viability of Snu449 wt and TP53INP2 KD cells after 25 ng/ml TRAIL treatment. Data are presented as mean ± SEM of four or five independent experiments.

Data information: Two-way Student's *t*-test was performed; $*P < 0.05$, $**P < 0.01$, $***P < 0.001$.
Source data are available online for this figure.

proteins work together to regulate skeletal muscle mass. In addition, TRAF6 has a regulatory role in amino acid starvation and mitophagy (Murata *et al*, 2013; Linares *et al*, 2015), raising the question as to whether TP53INP2 also has an adaptor role for TRAF6 in these two processes or more in general, which are the pathways that TRAF6 is involved in and might be modulated by TP53INP2.

As mentioned, TRAIL induces selective apoptosis in cancer cells (Ashkenazi *et al*, 1999; Walczak *et al*, 1999); however, this feature

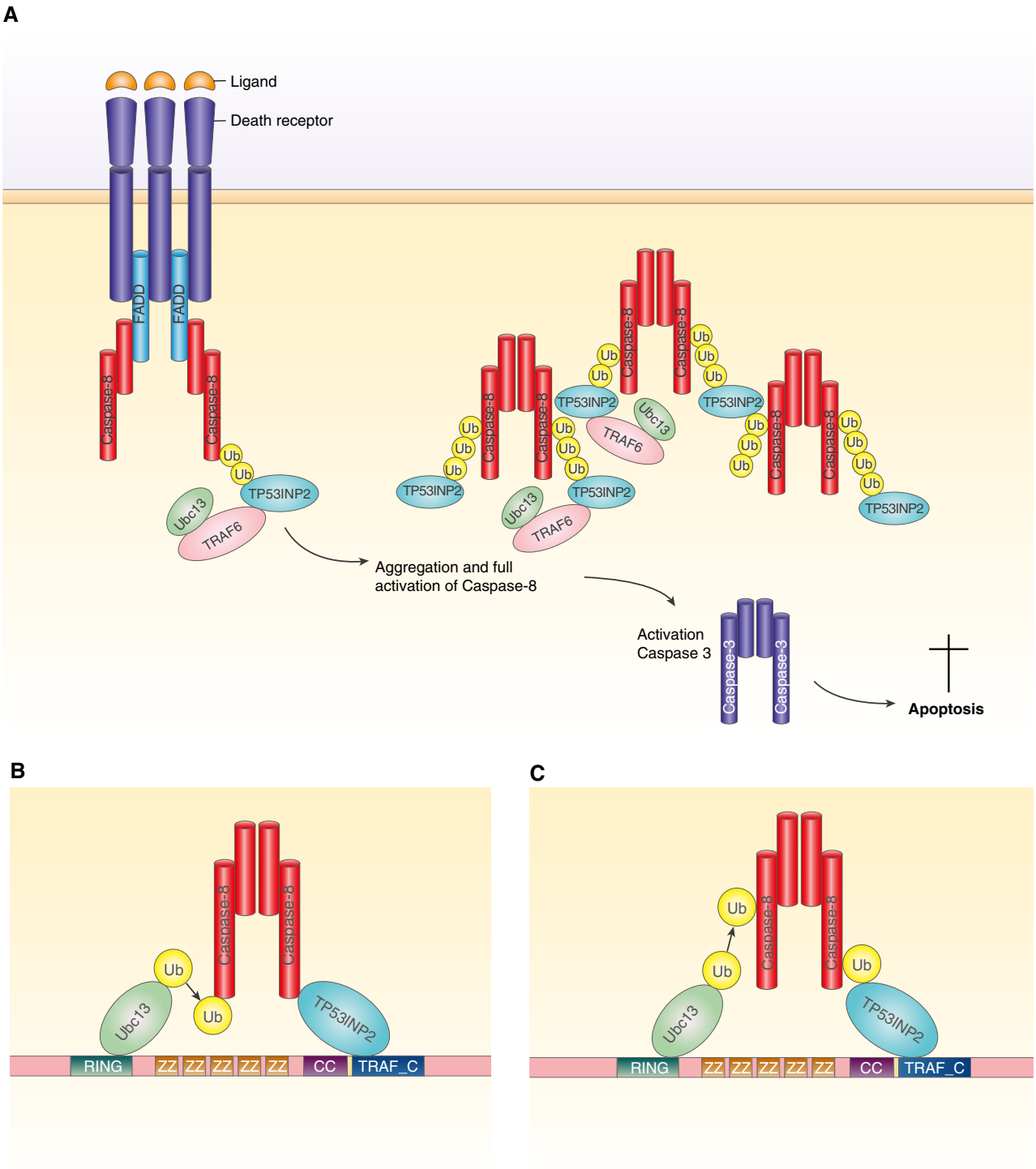

Figure 8. Model of TP53INP2 function in death receptor-induced apoptosis.

A Schematic presentation of TP53INP2 function in death receptor signaling. Upon receiving an upstream signal, the DISC complex is formed, where caspase-8 is recruited. TP53INP2 facilitates TRAF6 and caspase-8 complex and subsequent caspase-8 ubiquitination and activation.

B, C Proposed molecular mechanism of TP53INP2 in the ubiquitination of caspase-8 by TRAF6. E2 Ubc13 binds to the N-terminal RING and first ZZ domain of TRAF6, while TP53INP2 binds to the adaptor groove of the TRAF_C domain of TRAF6. In addition, TP53INP2 binds caspase-8 (B) and/or ubiquitinated caspase-8 (C), thus bringing caspase-8 and Ubc13 closer together for a more efficient ubiquitin transfer from Ubc13 to caspase-8. Since we could not make a mutant of TP53INP2 that cannot bind to ubiquitin, we cannot clearly discriminate between the two options. Our data indicate that TP53INP2 can bind to both forms of caspase-8 (non-ubiquitinated and ubiquitinated). However, binding is more efficient if caspase-8 is ubiquitinated, suggesting that TP53INP2 facilitates polyubiquitination of caspase-8 (C).

has not brought any benefit to cancer patients so far. There is a need for optimized TRAIL antagonists and strategies to tackle the resistance of tumors to TRAIL monotherapy. Furthermore, there is also a lack of biomarkers that can effectively identify patients likely to respond favorably to TRAIL-based therapy (Lemke *et al*, 2014b). To date, only one potential biomarker has been discovered. In this regard, CDK9 inhibition leads to the downregulation of two anti-apoptotic proteins, namely FLIP and MCL1, which act at the level of caspase-8 activation and mitochondria amplification of apoptosis (Lemke *et al*, 2014a). In addition, E-cadherin may also discriminate between the cells that respond to TRAIL therapy (Lu *et al*, 2014). Our results indicate that, by facilitating the ubiquitination and activation of caspase-8, TP53INP2 is another potential biomarker for TRAIL treatment (Fig 7). It would be interesting to see the expression of CDK9 in cancer cells with high levels of TP53INP2 and address whether CDK9 inhibition would synergistically increase sensitivity to TRAIL treatment. TRAIL therapy alone is clearly not effective. In this regard, it is important to simultaneously target several factors that cause TRAIL resistance and/or to increase the sensitivity of cancer cells to apoptosis. This strategy is critical since TRAIL administration could have pro-tumorigenic functions in some types of cancer, such as KRAS-mutated cancer (von Karstedt *et al*, 2015; Pal *et al*, 2016).

We report that TP53INP2 belongs to those proteins with dual functions in autophagy and apoptosis, which also include ATG5, ATG4D, Beclin 1, p62, and AMBRA1 among others (Yousefi *et al*, 2006; Cho *et al*, 2009; Laussmann *et al*, 2011; Huang *et al*, 2013; Strappazzon *et al*, 2016). TP53INP2 promotes autophagosomal formation and activates autophagy flux in different cell types (Nowak *et al*, 2009; Mauvezin *et al*, 2010; Sala *et al*, 2014; Romero *et al*, 2018). In this study, we show that TP53INP2 acts also as a switch at the level of caspase-8 activation, favoring death receptor-mediated apoptosis. This effect of TP53INP2 promoting caspase-8 activation does not require autophagy machinery, probably because TP53INP2 function in death receptor signaling is upstream from autophagy. Once caspase-8 is activated, it cleaves TP53INP2 at LIR sequence and prevents its role in autophagy, thus further promoting apoptosis and downregulating the pro-survival role of autophagy. It will be interesting to see how other stresses (not death ligands) influence TP53INP2 function in apoptosis/autophagy cross-talk.

Taken together, our data reveal an unexpected role of TP53INP2 in the regulation of death receptor signaling. The mechanism involves the scaffolding function of TP53INP2 and facilitates caspase-8 ubiquitination by TRAF6, thereby switching or shifting death receptor signaling toward apoptosis. This finding unveils an additional point of apoptosis regulation that can be explored in TRAIL therapy.

Materials and Methods

Plasmid constructs

We used following constructs: pCDNA3-FLAG-TP53INP2, pCMV-FLAG-TRAF6 was a gift from John Kyriakis (Addgene 21624), pCMV-FLAG-TRAF6 C70A, HA-Ub was a gift from Edward Yeh (Addgene 18712), His-Ub was a gift from Astar Winoto (Addgene 31815), HA-Ub K48 was a gift from Ted Dawson (Addgene 17605), HA-Ub K63 was a gift from Ted Dawson (Addgene17606), XPRESS-caspase-8-NCC (kind gift from A. Ashkenazi), FLAG-caspase-8 (kind gift from A. Ashkenazi), FLAG-caspase-8-Ub6 (kind gift from A. Ashkenazi), FLAG-caspase-8-Ub9 (kind gift from A. Ashkenazi), pCDNA3-TP53INP2, pCDNA3-TP53INP2 TIM mutant, pCDNA3-TP53INP2 3KR mutant, pCDNA3-TP53INP2 LIR mutant, pCDNA3-TP53INP2 3DE mutant, HA-p62 was a gift from Qing Zhong (Addgene 28027), and myc-caspase-3 C163A was a gift from Guy Salvesen (Addgene 11814). All mutations were done with the Quick Mutagenesis Kit by Promega, following the manufacturer's instructions, and the sequences were verified by DNA sequencing.

Cell culture

HeLa, HEK293T, MCF7, MDA-MB-231, MDA-MB-468, SKBr3, Huh7, PLC, Hep3B, and MEF TRAF6 KO (kind gift from Manolis Pasparakis) cells were grown in DMEM (Gibco) supplemented with 10% fetal bovine serum (FBS, Sigma); BT20 cells were grown in MEM supplemented with 10% FBS; T47D and BT474 cells were grown in RPMI (Gibco) supplemented with 10% FBS; and Snu449, HLE, and HLF cells were cultured in RPMI with 10% FBS and 1% NEAA (Sigma). Flp-In T-REx 293 cells expressing HA-FLAG-TP53INP2 were made following the manufacturer's instructions (Thermo Fisher Scientific). Staurosporine, doxorubicin, and actinomycin D were from Sigma, bafilomycin A1 from Santa Cruz, cisplatin from Ebewe Pharma, nec-1 from Enzo Life Sciences, z-VAD-fmk from Bachem, FasL and TNFα from Milipore, TRAIL from R&D Systems, and CHX from Calbiochem. Nec-1 and z-VAD-fmk were added 2 h before the induction of apoptosis.

Mouse model

The L-KO DOR mouse line was generated by crossing homozygous TP53INP2 loxP/loxP mice with a mouse strain expressing Cre recombinase under the control of the albumin promoter. Mice were in a C57BL/6J pure genetic background. Non-expressing Cre TP53INP2loxP/loxP littermates were used as controls for knockout animals. Twelve- to 16-week-old mice were used in all experiments. All animal experiments were done in compliance with guidelines established by the University of Barcelona Committee on Animal Care. Mice were kept under a 12-h dark–light period and provided with a standard chow-diet and water *ad libitum*. For FasL treatment, mice were injected i.p. with 0.15 μg/g body weight and sacrificed 4 h later. For doxorubicin (30 mg/kg body weight) and cisplatin (20 mg/kg body weight), mice were injected i.p. and sacrificed 48 h later.

Immunohistochemistry and immunofluorescence in liver sections

For immunohistochemistry and immunofluorescence assays, livers were fixed in PFA 4% o/n at room temperature. After two washes in PBS for 5 min, sections were incubated in NH_4Cl (50 mM) and glycine (20 mM) to reduce the autofluorescence and permeabilized by incubating them with a solution of 0.1% Triton X-100 in 0.1% sodium citrate for 2 min at 4°C. After two washes in PBS for 5 min and blocking during 30 min in 10% FBS in PBS, slides were incubated with Tom20 (Santa Cruz) and cytochrome c (BD Pharmingen) in blocking solution for 2 h. After three 10 min washes in PBS,

samples were further incubated in donkey anti-guinea pig Alexa-Fluor 568 conjugated secondary antibodies (Invitrogen) for 1 h, followed again by three 10 min washes in PBS. Hoechst33342 (1/2,000; Molecular Probes) was used to label DNA. Sections were kept in the dark after secondary antibody incubation. Slides were finally covered using Fluoromount (Sigma) and allowed to dry o/n before being stored at 4°C. A Leica TCS SP5 confocal scanning microscope was used to analyze the immunofluorescence. TUNEL staining to detect apoptosis was performed according to the manufacturer's instructions (In Situ Cell Death Detection Kit Fluorescein, Roche). For light microscopy, sections were stained with hematoxylin and eosin or cleaved caspase-3 following standard protocols.

Caspase-3 protein expression and cleavage assay

Recombinant caspase-3 was expressed in *Escherichia coli* and purified as described previously (Stennicke & Salvesen, 1999). Caspase cleavage assays were performed in 20 mM Hepes buffer, pH 7.2, containing 100 mM NaCl, 10 mM dithiothreitol, 1 mM EDTA, 0.1 (w/v) CHAPS, and 10% (w/v) sucrose at 37°C. Briefly, caspases were incubated for 5 min in the reaction buffer at 37°C prior to the addition of lysates overexpressing wild-type TP53INP2 or 3DE mutant to the final volume of 25 μl. The final concentration of caspases was 1 μM. After 1-h incubation with caspases, the reactions were terminated by the addition of l× SDS loading buffer and boiling. The reaction mixtures were analyzed by 12% SDS–PAGE gels and Western blot.

Immunoblotting

Cells were collected at the times indicated in the text post-induction of apoptosis and incubated in RIPA buffer [50 mM Tris (pH 8.0), 100 mM NaCl, 0.1% (w/v) SDS, 1% (v/v) Nonident P-40, 0.5% (w/v) deoxycholic acid, 1 mM EDTA] for 10 min on ice. Insoluble material was removed by centrifugation at 18,000 *g* for 10 min. Pierce assay (Promega) was used to determine protein concentration, and 50 μg of protein was resolved in 10 or 12% SDS–PAGE gels. After transfer to PVDF membrane (Millipore), blots were probed with antibodies against PARP (Cell Signaling), caspase-3 (Cell Signaling), cleaved caspase-3 (Cell Signaling), caspase-8 (Cell Signaling, BD Pharmingen), p62 (Progen), DR4 (Cell Signaling), DR5 (Cell Signaling), LC3 (MBL International), TP53INP2 (made in our laboratory), TRAF6 (Cell Signaling), FLAG (Sigma), XPRESS (Invitrogen), Bcl-2 (Santa Cruz), Bid (Cell Signaling), Mcl-1 (Cell signaling), Bcl-xl (Santa cruz), Bak (Santa Cruz), Bax (Cell Signaling), actin (Sigma), myc (Santa Cruz), and appropriate HRP-conjugated secondary antibodies (Jackson) and visualized with ECL following the manufacturer's instructions (Amersham). Cell fractionation was done with NE-PER Nuclear and Cytoplasmic Extraction Reagents Kit (Thermo Fisher) following manufacturer's instructions.

Immunoprecipitation and pull-down assay

Cells were transfected with the indicated plasmids with polyethyleneimine (PEI) from Polysciences Inc., lysed for 36 h after transfection in lysis buffer and subjected to pull-down assays with FLAG (Sigma), Nickel (Invitrogen), or HA (Sigma) resin, following the manufacturer's instructions. For denaturing pull-down, 6 M urea was added to the lysis buffer. Immunocomplexes were separated by SDS–PAGE and detected by Western blot analysis. For endogenous immunoprecipitation, cells were incubated or not with 100 ng/ml of TRAIL for 30 min. Afterward, cells were cross-linked with formaldehyde (PanReac AppliChem) for 10 min, scraped and washed with PBS. Cell lysis was performed with FLAG lysis buffer, and supernatants were added to the protein G sepharose beads (Sigma) previously incubated with normal mouse IgG (Sigma) or anti-caspase-8 mouse antibody (BD Pharmingen). Primary antibodies were cross-linked to protein G sepharose by DMP (Thermo Fisher) following manufacturer's instructions, and immunocomplexes were eluted with glycine (pH = 3). For recombinant proteins pull-downs, FLAG-caspase-8, TP53INP2, and FLAG-TP53INP2 were *in vitro* translated with Promega's TNT *in vitro* translation system and GST (Abcam) and GST-TRAF6 (Abnova) were purchased. Recombinant proteins were subjected to pull-down with FLAG (Sigma) resin, following manufacturer's instructions.

DEVDase activity and FACS analysis

30 μg of protein of untreated and treated cells in the presence or absence of inhibitors was used to determine caspase activity by measuring the cleavage of fluorogenic substrate Ac-DEVD-AFC (Bachem) using Tecan.

For flow cytometry, cells were harvested at the indicated times after treatment. Culture medium supernatant and PBS washes were retained to ensure that both floating and adherent cells were analyzed. After incubation for 15 min with Annexin V Alexa-647 (Invitrogen) following the manufacturer's instructions, and propidium iodide, cells were subjected to FACS analysis.

Fluorescence microscopy

Cells grown on coverslips for the indicated treatments were washed with PBS and fixed in 4% paraformaldehyde (Santa Cruz) for 10 min, followed by permeabilization with 0.2% (v/v) Triton X-100 in PBS for 15 min. After extensive washing with PBS, cells were incubated with primary antibodies for 1 h on room temperature. Following an additional round of extensive washing with PBS, cells were incubated either with goat anti-rabbit Alexa-647 or goat anti-mouse Alexa-488 antibody (Molecular Probes) for 60 min at room temperature. After incubation, cells were washed with PBS, mounted on slides with Fluoromount (Sigma), and visualized by confocal microscope (Leica). Hoechst (Sigma) was used to stain the nuclei. For live cell imaging, HeLa cells were transfected with TP53INP2-RFP and wide-field images of live cells were captured using an Olympus 1X81 microscope in an imaging chamber with CO_2 and temperature control. Scans were taken every 5 min for approximately 3 h. TRAIL (100 ng/ml) was added after second frame was taken.

Knock-down and CRISPR technology

HeLa cells were transfected with lentiviruses with shRNA for ATG5, p62, and caspase-8 with PEI, and 48 h after exposed to puromycin selection. The level of knock-down was analyzed by Western blot. To knock out TRAF6, ATG7, and TP53INP2, we used a CRISPR technology. For TRAF6 and TP53INP2, the CRISPR plasmids were

bought from Santa Cruz and done according to manufacturer's instructions. Forward and reverse oligonucleotides containing the guide sequence to Atg7 (Forward 1: CACCGGAAGCTGAACGAGTAT CGGC, Reverse 1: AAACGCCGATACTCGTTCAGCTTCC; Forward 2: CACCGAACTCCAATGTTAAGCGAGC; Reverse 2: AAACGCTCGCT TAACATTGGAGTTC) and TP53INP2 (Forward 1: CACCGCTCTGGT TCTTGGACCGGCG, Reverse 1: AAACCGCCGGTCCAAGAACCAGA GC; Forward 2: CACCGACCGGCGCGGACGGCTCTCG; Reverse 2: A AACCGAGAG CCGTCCGCGC CGGTC) were annealed and cloned into the pX330 plasmid (Cong *et al*, 2013) that was subsequently transfected into HeLa cells using NanoJuice (NanoJuice™ Transfection Kit, Novagen). GFP-positive cells were sorted 24 h after transfection (BD FACSAria III SORP) and grown as single clones. Screening for Atg7-KO and TP53INP2-KO cells was carried out by Western blotting.

In vitro ubiquitination

In vitro ubiquitination assays were performed with the following components: immunoprecipitated XPRESS-caspase-8-NCC, FLAG-TP53INP2 and FLAG-TRAF6 (E3), UbcH13 (E2) and ubiquitin activating kit (Enzo), following the manufacturer's instructions.

Statistics

Microsoft Office Excel was used for data analysis. Student's *t*-tests were used to compare results between two groups. Data were presented as mean with standard error of the mean (SEM). *P*-values < 0.05 were considered significant.

Expanded View for this article is available online.

Acknowledgements
The XPRESS-caspase-8-NCC, wt FLAG-caspase-8, and Ub6 and Ub9 constructs were generous gifts from Avi Ashkenazi (Genentech, USA). MEF TRAF6 KO cells were obtained from Manolis Pasparakis (Koln, Germany). We thank Vanessa Hernández and Jorge Manuel Seco for technical assistance; Anna Llado and Lidia Bardia from Advanced Digital Microscopy (IRB Barcelona) for help with confocal microscopy experiments and analysis; Histopathology Facility (IRB Barcelona) for immunohistochemistry staining of liver samples; and Flow cytometry facility (PCB Barcelona) for help with flow cytometry experiments. A.Z. is a recipient of an ICREA "Academia" (Generalitat de Catalunya), and S.I. is a researcher hired by CIBERDEM (Instituto de Salud Carlos III). C.B. was supported by the Deutsche Forschungsgemeinschaft (DFG) within the framework of the Munich Cluster for Systems Neurology (EXC2145 SyNergy) and the Collaborative Research Center (CRC1177) as well as by the Boehringer Ingelheim Foundation. This study was supported by research grants from the MINECO (SAF2013-40987R and SAF2016-75246R), the Generalitat de Catalunya (Grant 2014SGR48), Fundació la Marató de TV3 (20132330), CIBERDEM ("Instituto de Salud Carlos III"), INTERREG IV-B-SUDOE-FEDER (DIOMED, SOE1/P1/E178); and "la Caixa" Foundation (LCF/PR/GN14/10270002). We gratefully acknowledge institutional funding from the MINECO through the Centres of Excellence Severo Ochoa Award, and from the CERCA Programme of the Generalitat de Catalunya.

Author contributions
SI designed and executed the experiments and wrote manuscript; MP made TP53INP2-overexpressing cell models; AJN-P made TP53INP2 and TRAF6 KD or KO in MDA231 cells and helped with revision experiments; MIH-A helped with L-KO mice generation and *in vivo* FasL experiments; PF made TP53INP2 KD in Snu449 cells and cell fractionation experiments; KS made ATG7 KO cells and TP53INP2 CRISPR vectors; NP helped with L-KO mice generation; ARN and MP discussed the results and helped with manuscript writing; RRG and CB discussed the data and helped with design of some experiments; and AZ helped with the design of the experiments, discussed the data, and helped with manuscript writing.

Conflict of interest
The authors declare that they have no conflict of interest.

References

Ashkenazi A, Pai RC, Fong S, Leung S, Lawrence DA, Marsters SA, Blackie C, Chang L, McMurtrey AE, Hebert A, DeForge L, Koumenis IL, Lewis D, Harris L, Bussiere J, Koeppen H, Shahrokh Z, Schwall RH (1999) Safety and antitumor activity of recombinant soluble Apo2 ligand. *J Clin Invest* 104: 155 – 162

Baumgartner BG, Orpinell M, Duran J, Ribas V, Burghardt HE, Bach D, Villar AV, Paz JC, Gonzalez M, Camps M, Oriola J, Rivera F, Palacin M, Zorzano A (2007) Identification of a novel modulator of thyroid hormone receptor-mediated action. *PLoS One* 2: e1183

Bell BD, Leverrier S, Weist BM, Newton RH, Arechiga AF, Luhrs KA, Morrissette NS, Walsh CM (2008) FADD and caspase-8 control the outcome of autophagic signaling in proliferating T cells. *Proc Natl Acad Sci USA* 105: 16677 – 16682

Bhattacharya A, Schmitz U, Raatz Y, Schonherr M, Kottek T, Schauer M, Franz S, Saalbach A, Anderegg U, Wolkenhauer O, Schadendorf D, Simon JC, Magin T, Vera J, Kunz M (2015) miR-638 promotes melanoma metastasis and protects melanoma cells from apoptosis and autophagy. *Oncotarget* 6: 2966 – 2980

Cho DH, Jo YK, Hwang JJ, Lee YM, Roh SA, Kim JC (2009) Caspase-mediated cleavage of ATG6/Beclin-1 links apoptosis to autophagy in HeLa cells. *Cancer Lett* 274: 95 – 100

Cong L, Ran FA, Cox D, Lin S, Barretto R, Habib N, Hsu PD, Wu X, Jiang W, Marraffini LA, Zhang F (2013) Multiplex genome engineering using CRISPR/Cas systems. *Science (New York, NY)* 339: 819 – 823

Deegan S, Saveljeva S, Logue SE, Pakos-Zebrucka K, Gupta S, Vandenabeele P, Bertrand MJ, Samali A (2014) Deficiency in the mitochondrial apoptotic pathway reveals the toxic potential of autophagy under ER stress conditions. *Autophagy* 10: 1921 – 1936

Dickens LS, Boyd RS, Jukes-Jones R, Hughes MA, Robinson GL, Fairall L, Schwabe JW, Cain K, Macfarlane M (2012) A death effector domain chain DISC model reveals a crucial role for caspase-8 chain assembly in mediating apoptotic cell death. *Mol Cell* 47: 291 – 305

Duran A, Hernandez ED, Reina-Campos M, Castilla EA, Subramaniam S, Raghunandan S, Roberts LR, Kisseleva T, Karin M, Diaz-Meco MT, Moscat J (2016) p62/SQSTM1 by binding to vitamin D receptor inhibits hepatic stellate cell activity, fibrosis, and liver cancer. *Cancer Cell* 30: 595 – 609

Ferri KF, Kroemer G (2001) Mitochondria–the suicide organelles. *BioEssays* 23: 111 – 115

Francis VA, Zorzano A, Teleman AA (2010) dDOR is an EcR coactivator that forms a feed-forward loop connecting insulin and ecdysone signaling. *Curr Biol* 20: 1799 – 1808

Fulda S, Debatin KM (2006) Extrinsic versus intrinsic apoptosis pathways in anticancer chemotherapy. *Oncogene* 25: 4798 – 4811

Giansanti V, Torriglia A, Scovassi AI (2011) Conversation between apoptosis and autophagy: "Is it your turn or mine?". *Apoptosis* 16: 321 – 333

Gonzalvez F, Lawrence D, Yang B, Yee S, Pitti R, Marsters S, Pham VC, Stephan JP, Lill J, Ashkenazi A (2012) TRAF2 Sets a threshold for extrinsic apoptosis by tagging caspase-8 with a ubiquitin shutoff timer. *Mol Cell* 48: 888 – 899

Hartwig T, Montinaro A, von Karstedt S, Sevko A, Surinova S, Chakravarthy A, Taraborrelli L, Draber P, Lafont E, Arce Vargas F, El-Bahrawy MA, Quezada SA, Walczak H (2017) The TRAIL-induced cancer secretome promotes a tumor-supportive immune microenvironment via CCR2. *Mol Cell* 65: 730 – 742

He L, Wu X, Siegel R, Lipsky PE (2006) TRAF6 regulates cell fate decisions by inducing caspase 8-dependent apoptosis and the activation of NF-kappaB. *J Biol Chem* 281: 11235 – 11249

Henry CM, Martin SJ (2017) Caspase-8 acts in a non-enzymatic role as a scaffold for assembly of a pro-inflammatory "FADDosome" complex upon TRAIL stimulation. *Mol Cell* 65: 715 – 729

Huang S, Okamoto K, Yu C, Sinicrope FA (2013) p62/sequestosome-1 up-regulation promotes ABT-263-induced caspase-8 aggregation/activation on the autophagosome. *J Biol Chem* 288: 33654 – 33666

Huang R, Xu Y, Wan W, Shou X, Qian J, You Z, Liu B, Chang C, Zhou T, Lippincott-Schwartz J, Liu W (2015) Deacetylation of nuclear LC3 drives autophagy initiation under starvation. *Mol Cell* 57: 456 – 466

Jacobson MD, Weil M, Raff MC (1999) Programmed cell death in animal development. *Cell* 88: 347 – 354

Jadhav TS, Wooten MW, Wooten MC (2011) Mining the TRAF6/p62 interactome for a selective ubiquitination motif. *BMC Proc* 28: 1753 – 6561

Jiang H, White EJ, Rios-Vicil CI, Xu J, Gomez-Manzano C, Fueyo J (2011) Human adenovirus type 5 induces cell lysis through autophagy and autophagy-triggered caspase activity. *J Virol* 85: 4720 – 4729

Jin Z, Li Y, Pitti R, Lawrence D, Pham VC, Lill JR, Ashkenazi A (2009) Cullin3-based polyubiquitination and p62-dependent aggregation of caspase-8 mediate extrinsic apoptosis signaling. *Cell* 137: 721 – 735

von Karstedt S, Conti A, Nobis M, Montinaro A, Hartwig T, Lemke J, Legler K, Annewanter F, Campbell AD, Taraborrelli L, Grosse-Wilde A, Coy JF, El-Bahrawy MA, Bergmann F, Koschny R, Werner J, Ganten TM, Schweiger T, Hoetzenecker K, Kenessey I *et al* (2015) Cancer cell-autonomous TRAIL-R signaling promotes KRAS-driven cancer progression, invasion, and metastasis. *Cancer Cell* 27: 561 – 573

von Karstedt S, Montinaro A, Walczak H (2017) Exploring the TRAILs less travelled: TRAIL in cancer biology and therapy. *Nat Rev Cancer* 17: 352 – 366

Kreuz S, Siegmund D, Scheurich P, Wajant H (2001) NF-kappaB inducers upregulate cFLIP, a cycloheximide-sensitive inhibitor of death receptor signaling. *Mol Cell Biol* 21: 3964 – 3973

Kruse R, Vind BF, Petersson SJ, Kristensen JM, Hojlund K (2015) Markers of autophagy are adapted to hyperglycaemia in skeletal muscle in type 2 diabetes. *Diabetologia* 58: 2087 – 2095

Laussmann MA, Passante E, Dussmann H, Rauen JA, Wurstle ML, Delgado ME, Devocelle M, Prehn JH, Rehm M (2011) Proteasome inhibition can induce an autophagy-dependent apical activation of caspase-8. *Cell Death Differ* 18: 1584 – 1597

Lemke J, von Karstedt S, Abd El Hay M, Conti A, Arce F, Montinaro A, Papenfuss K, El-Bahrawy MA, Walczak H (2014a) Selective CDK9 inhibition overcomes TRAIL resistance by concomitant suppression of cFlip and Mcl-1. *Cell Death Differ* 21: 491 – 502

Lemke J, von Karstedt S, Zinngrebe J, Walczak H (2014b) Getting TRAIL back on track for cancer therapy. *Cell Death Differ* 21: 1350 – 1364

Li H, Zhu H, Xu CJ, Yuan J (1998) Cleavage of BID by caspase 8 mediates the mitochondrial damage in the Fas pathway of apoptosis. *Cell* 94: 491 – 501

Li Y, Kong Y, Zhou Z, Chen H, Wang Z, Hsieh YC, Zhao D, Zhi X, Huang J, Zhang J, Li H, Chen C (2013) The HECTD3 E3 ubiquitin ligase facilitates cancer cell survival by promoting K63-linked polyubiquitination of caspase-8. *Cell Death Dis* 28: 464

Li RF, Chen G, Ren JG, Zhang W, Wu ZX, Liu B, Zhao Y, Zhao YF (2014) The adaptor protein p62 is involved in RANKL-induced autophagy and osteoclastogenesis. *J Histochem Cytochem* 62: 879 – 888

Linares GR, Xing W, Burghardt H, Baumgartner B, Chen ST, Ricart W, Fernandez-Real JM, Zorzano A, Mohan S (2011) Role of diabetes- and obesity-related protein in the regulation of osteoblast differentiation. *Am J Physiol Endocrinol Metab* 301: 5

Linares JF, Duran A, Reina-Campos M, Aza-Blanc P, Campos A, Moscat J, Diaz-Meco MT (2015) Amino acid activation of mTORC1 by a PB1-domain-driven kinase complex cascade. *Cell Rep* 12: 1339 – 1352

Long M, Li X, Li L, Dodson M, Zhang DD, Zheng H (2017) Multifunctional p62 effects underlie diverse metabolic diseases. *Trends Endocrinol Metab* 28: 818 – 830

Lu M, Marsters S, Ye X, Luis E, Gonzalez L, Ashkenazi A (2014) E-cadherin couples death receptors to the cytoskeleton to regulate apoptosis. *Mol Cell* 54: 987 – 998

Luo X, Budihardjo I, Zou H, Slaughter C, Wang X (1998) Bid, a Bcl2 interacting protein, mediates cytochrome c release from mitochondria in response to activation of cell surface death receptors. *Cell* 94: 481 – 490

Mauvezin C, Orpinell M, Francis VA, Mansilla F, Duran J, Ribas V, Palacin M, Boya P, Teleman AA, Zorzano A (2010) The nuclear cofactor DOR regulates autophagy in mammalian and *Drosophila* cells. *EMBO Rep* 11: 37 – 44

Mauvezin C, Sancho A, Ivanova S, Palacin M, Zorzano A (2012) DOR undergoes nucleo-cytoplasmic shuttling, which involves passage through the nucleolus. *FEBS Lett* 586: 3179 – 3186

McManus S, Roux S (2012) The adaptor protein p62/SQSTM1 in osteoclast signaling pathways. *J Mol Signal* 7: 1750 – 2187

Medema JP, Scaffidi C, Kischkel FC, Shevchenko A, Mann M, Krammer PH, Peter ME (1997) FLICE is activated by association with the CD95 death-inducing signaling complex (DISC). *EMBO J* 16: 2794 – 2804

de Miguel D, Lemke J, Anel A, Walczak H, Martinez-Lostao L (2016) Onto better TRAILs for cancer treatment. *Cell Death Differ* 23: 733 – 747

Moscat J, Diaz-Meco MT (2009) p62 at the crossroads of autophagy, apoptosis, and cancer. *Cell* 137: 1001 – 1004

Murata H, Sakaguchi M, Kataoka K, Huh NH (2013) SARM1 and TRAF6 bind to and stabilize PINK1 on depolarized mitochondria. *Mol Biol Cell* 24: 2772 – 2784

Murphy JM, Czabotar PE, Hildebrand JM, Lucet IS, Zhang JG, Alvarez-Diaz S, Lewis R, Lalaoui N, Metcalf D, Webb AI, Young SN, Varghese LN, Tannahill GM, Hatchell EC, Majewski IJ, Okamoto T, Dobson RC, Hilton DJ, Babon JJ, Nicola NA *et al* (2013) The pseudokinase MLKL mediates necroptosis via a molecular switch mechanism. *Immunity* 39: 443 – 453

Naoum GE, Buchsbaum DJ, Tawadros F, Farooqi A, Arafat WO (2017) Journey of TRAIL from bench to bedside and its potential role in immuno-oncology. *Oncol Rev* 11: 3

Nowak J, Archange C, Tardivel-Lacombe J, Pontarotti P, Pebusque MJ, Vaccaro MI, Velasco G, Dagorn JC, Iovanna JL (2009) The TP53INP2 protein is required for autophagy in mammalian cells. *Mol Biol Cell* 20: 870 – 881

Pal S, Amin PJ, Sainis KB, Shankar BS (2016) Potential role of TRAIL in metastasis of mutant KRAS expressing lung adenocarcinoma. *Cancer Microenviron* 9: 77 – 84

Pan JA, Ullman E, Dou Z, Zong WX (2011) Inhibition of protein degradation induces apoptosis through a microtubule-associated protein 1 light chain 3-mediated activation of caspase-8 at intracellular membranes. *Mol Cell Biol* 31: 3158 – 3170

Pankiv S, Clausen TH, Lamark T, Brech A, Bruun JA, Outzen H, Overvatn A, Bjorkoy G, Johansen T (2007) p62/SQSTM1 binds directly to Atg8/LC3 to facilitate degradation of ubiquitinated protein aggregates by autophagy. *J Biol Chem* 282: 24131 – 24145

Paul PK, Kumar A (2011) TRAF6 coordinates the activation of autophagy and ubiquitin-proteasome systems in atrophying skeletal muscle. *Autophagy* 7: 555 – 556

Romero M, Sabate-Perez A, Francis VA, Castrillon-Rodriguez I, Diaz-Ramos A, Sanchez-Feutrie M, Duran X, Palacin M, Moreno-Navarrete JM, Gustafson B, Hammarstedt A, Fernandez-Real JM, Vendrell J, Smith U, Zorzano A (2018) TP53INP2 regulates adiposity by activating beta-catenin through autophagy-dependent sequestration of GSK3beta. *Nat Cell Biol* 20: 443 – 454

Sala D, Ivanova S, Plana N, Ribas V, Duran J, Bach D, Turkseven S, Laville M, Vidal H, Karczewska-Kupczewska M, Kowalska I, Straczkowski M, Testar X, Palacin M, Sandri M, Serrano AL, Zorzano A (2014) Autophagy-regulating TP53INP2 mediates muscle wasting and is repressed in diabetes. *J Clin Invest* 124: 1914 – 1927

Sancho A, Duran J, Garcia-Espana A, Mauvezin C, Alemu EA, Lamark T, Macias MJ, DeSalle R, Royo M, Sala D, Chicote JU, Palacin M, Johansen T, Zorzano A (2012) DOR/Tp53inp2 and Tp53inp1 constitute a metazoan gene family encoding dual regulators of autophagy and transcription. *PLoS One* 7: e34034

Schleich K, Warnken U, Fricker N, Ozturk S, Richter P, Kammerer K, Schnolzer M, Krammer PH, Lavrik IN (2012) Stoichiometry of the CD95 death-inducing signaling complex: experimental and modeling evidence for a death effector domain chain model. *Mol Cell* 47: 306 – 319

Shi Z, Zhang Z, Wang Y, Li C, Wang X, He F, Sun L, Jiao S, Shi W, Zhou Z (2015) Structural insights into mitochondrial antiviral signaling protein (MAVS)-tumor necrosis factor receptor-associated factor 6 (TRAF6) signaling. *J Biol Chem* 290: 26811 – 26820

Stennicke HR, Salvesen GS (1999) Caspases: preparation and characterization. *Methods* 17: 313 – 319

Strappazzon F, Di Rita A, Cianfanelli V, D'Orazio M, Nazio F, Fimia GM, Cecconi F (2016) Prosurvival AMBRA1 turns into a proapoptotic BH3-like protein during mitochondrial apoptosis. *Autophagy* 12: 963 – 975

Sugiyama M, Yoshizumi T, Yoshida Y, Bekki Y, Matsumoto Y, Yoshiya S, Toshima T, Ikegami T, Itoh S, Harimoto N, Okano S, Soejima Y, Shirabe K, Maehara Y (2017) p62 promotes amino acid sensitivity of mTOR pathway and hepatic differentiation in adult liver stem/progenitor cells. *J Cell Physiol* 232: 2112 – 2124

Tang Z, Takahashi Y, Chen C, Liu Y, He H, Tsotakos N, Serfass JM, Gebru MT, Chen H, Young MM, Wang HG (2017) Atg2A/B deficiency switches cytoprotective autophagy to non-canonical caspase-8 activation and apoptosis. *Cell Death Differ* 24: 2127 – 2138

Tummers B, Green DR (2017) Caspase-8: regulating life and death. *Immunol Rev* 277: 76 – 89

Vaux DL, Korsmeyer SJ (1999) Cell death in development. *Cell* 96: 245 – 254

Walczak H, Miller RE, Ariail K, Gliniak B, Griffith TS, Kubin M, Chin W, Jones J, Woodward A, Le T, Smith C, Smolak P, Goodwin RG, Rauch CT, Schuh JC, Lynch DH (1999) Tumoricidal activity of tumor necrosis factor-related apoptosis-inducing ligand *in vivo*. *Nat Med* 5: 157 – 163

Walsh MC, Lee J, Choi Y (2015) Tumor necrosis factor receptor- associated factor 6 (TRAF6) regulation of development, function, and homeostasis of the immune system. *Immunol Rev* 266: 72 – 92

Wooff J, Pastushok L, Hanna M, Fu Y, Xiao W (2004) The TRAF6 RING finger domain mediates physical interaction with Ubc13. *FEBS Lett* 566: 229 – 233

Xu Y, Wan W, Shou X, Huang R, You Z, Shou Y, Wang L, Zhou T, Liu W (2016) TP53INP2/DOR, a mediator of cell autophagy, promotes rDNA transcription via facilitating the assembly of the POLR1/RNA polymerase I preinitiation complex at rDNA promoters. *Autophagy* 12: 1118 – 1128

Ye H, Arron JR, Lamothe B, Cirilli M, Kobayashi T, Shevde NK, Segal D, Dzivenu OK, Vologodskaia M, Yim M, Du K, Singh S, Pike JW, Darnay BG, Choi Y, Wu H (2002) Distinct molecular mechanism for initiating TRAF6 signalling. *Nature* 418: 443 – 447

Young MM, Takahashi Y, Khan O, Park S, Hori T, Yun J, Sharma AK, Amin S, Hu CD, Zhang J, Kester M, Wang HG (2012) Autophagosomal membrane serves as platform for intracellular death-inducing signaling complex (iDISC)-mediated caspase-8 activation and apoptosis. *J Biol Chem* 287: 12455 – 12468

Yousefi S, Perozzo R, Schmid I, Ziemiecki A, Schaffner T, Scapozza L, Brunner T, Simon HU (2006) Calpain-mediated cleavage of Atg5 switches autophagy to apoptosis. *Nat Cell Biol* 8: 1124 – 1132

Zou H, Li Y, Liu X, Wang X (1999) An APAF-1.cytochrome c multimeric complex is a functional apoptosome that activates procaspase-9. *J Biol Chem* 274: 11549 – 11556